FATIGUE ANALYSIS OF ARTERIES USING FINITE ELEMENT METHOD

A Thesis
Submitted to the Graduate Faculty
Of the
North Dakota State University
Of Agriculture and Applied Science

By

Rusha Banerjee

In Partial Fulfillment of the Requirements
For the Degree of
MASTER OF SCIENCE

Major Department:
Mechanical Engineering

September 2012

Fargo, North Dakota

North Dakota State University
Graduate School

Title

Fatigue Analysis of Arteries Using

Finite Element Method

By

Rusha Banerjee

The Supervisory Committee certifies that this *disquisition* complies with North Dakota State University's regulations and meets the accepted standards for the degree of

MASTER OF SCIENCE

SUPERVISORY COMMITTEE:

Dr. Ghodrat Karami

Co-Chair

Dr. Fardad Azarmi

Co-Chair

Dr. Mariusz Ziejewski

Dr. Eakalak Khan

Approved by Department Chair:

1/22/2013 Dr. Alan Kallmeyer

Signature

ABSTRACT

In this thesis, the fatigue response of arteries to four specific physiological conditions representative of various morphological changes that artery undergo during its lifetime, was explored. Single layered nonlinear elastic micromechanical model of artery was developed for this purpose.

A comparative study was completed on fatigue response, in the form of available life and shear stress accumulation, between hypertensive and normotensive arteries.

The effects of morphological changes of ageing arteries on the fatigue response of the artery were studied. Change in stiffness, arterial dilation and remodeling were taken into consideration.

The effect of undulation of the artery, due to weakening of arterial walls with age or hypertension, on fatigue response, is the third aspect of this study.

Lastly, the contribution of the surrounding linear elastic tissue material on fatigue response of the artery was investigated to reflect the in-vivo condition of artery where it is always surrounded by different tissues.

ACKNOWLEDGMENTS

I would like to extend my gratitude to my academic advisor, Dr. Ghodrat Karami and co-advisor Dr Fardad Azarmi, for their guidance and support throughout the tenure of my research work. Their valuable advice, experience, criticism and encouragement have all helped me develop my research skills, fully utilize my technical expertise, be more innovative, and improve my problem solving skills.

I would also like to thank the members of my supervisory committee, Dr Mariusz Ziejewski and Dr Eakalak Khan for taking time out of their busy schedules to provide me with continuous support, and advice, on my research work. I am grateful to Dr Alan Kallmeyer, Chair of the Department of Mechanical Engineering, NDSU, as well, for his valuable advice and support throughout my tenure as a graduate student in the Department.

TABLE OF CONTENTS

LIST OF TABLES

LIST OF FIGURES

CHAPTER 1. INTRODUCTION

1.1. Research objective and justification

The primary objective of this study is to utilize finite element to predict the fatigue response of the arteries under various physiological conditions that the artery encounters during its lifetime. The artery during its lifetime is continuously subjected to cyclic loading in the form of pulsating blood pressure. Although the extent of the pressure is usually within physiological limit and not very high, the transient loading results in the development of residual stress within the artery. The soft tissue of the artery accumulates damage at every load cycle and depending upon the structural stability of the artery the accumulated damage can eventually lead to the failure of the artery before the stress levels within the artery reach its yield limit. Hence it is important to understand the actual properties and state of the artery when predicting its life.

Four different aspects of fatigue response were analyzed in this study. The first part of the parametric study is aimed at analyzing the fatigue response of arteries under hypertension with a variation in mechanical properties. Hypertension is the condition when the pressure of the blood flowing through the artery increases beyond the normal range. Progressive weakening of the arteries with age causes greater stress to develop on the arterial wall. Development of plaques on the inner arterial wall resulting in constriction of the artery diameter also contributes to increased blood pressure within the artery. Hypertension is accompanied by arterial dilation along with an increase in wall stiffness. For this study it was assumed that the internal diameters and thickness of both normotensive and hypertensive arteries were similar. Fatigue analysis of the arteries under hypertension becomes critical when studying arteries subjected to ailments like aneurysms and

arthrosclerosis. Aneurysm is the condition when the arterial wall balloons at the weak spots, stretching the arterial wall and decreasing its thickness greatly. The aneurysms tend to burst before the end of its predicted life based on yield stress of arteries due to fatigue damage accumulation. Moreover hypertension accelerates the process of degeneration. Similarly arthrosclerosis results in the development of higher stress levels within the arterial wall resulting in the development of weak spots which service as the areas of maximum fatigue damage accumulation.

In the second part of the parametric study involving the study of the effect of age on the fatigue response of male coronary arteries, arterial remodeling in the form of variation in arterial stiffness, external diameters and thickness of artery were all taken into account. Shear stress development and its effect on the fatigue life of an artery were analyzed in the study. With age the arterial architecture and properties change, arteries become stiffer and the arterial lumen have been observed to decrease in diameter with age. Higher stress accumulation due to increased stiffness of the arteries combined with the effect of arterial remodeling affects the response of the arteries to transient blood pressure for different age groups.

Arterial undulation is a phenomenon which has been observed to occur under various abnormal conditions. Pressure variations within the artery in the form of hypertension; or loss of pressure and morphological changes in the artery due to ageing, or disease, leading to reduced arterial stiffness and weakened arterial wall, may lead to arterial undulation. The effect of the deformation in the arterial structure on its mechanical response has not yet been previously analyzed. This study aimed at analyzing the stress concentration patterns due to undulations developed in the artery and the subsequent effect on fatigue life by developing

an FE model for an undulated artery. Undulations in the arterial wall may result in the development of notches or crevices, areas of high stress concentration. These areas may later develop into weak spots where fatigue failure is usually initiated.

The artery functions under different types of physiological pressures in vivo like that of surrounding tissue material, or organs. It becomes crucial, therefore, to understand the effect of this factor on the fatigue response of the artery. Tissue material mimicking gelatin was used to understand the effect of the surrounding stiffness on the mechanical properties like Young's modulus of the artery. In this FE study, the surrounding tissue material was modeled as an elastic material for computational simplicity and its effect of the fatigue response of the artery was observed.

The results are expressed in form shear stress plot and fatigue life. Maximum shear stress developed in the artery is a critical factor in determining the life of the artery. The constant physiological cyclic loading of the blood pressure within the artery results in the development of shear and normal stress within the walls of the artery. The pressure on the inner face of the artery is higher than that on the outer face which brings into effect a shear force between the walls of the artery. Normal stress developed in the artery in the perpendicular directions is low since the blood pressure is under physiological limits and over a the life time of the artery it's the effect of the shear stress that results in the development of fatigue damage within the artery.

1.2. Background study

1.2.1. Insight into fatigue analysis

Fatigue is the progressive accumulation of damage, and eventual failure, of material subjected to cyclic loading. Deformation, and eventual fracture of materials, has been an area of research and study since the nineteenth century. There are two specific approaches that are adopted when any kind of fatigue analysis is being conducted: 1) stress life, or high cycle, fatigue analysis and 2) strain-life, or low cycle, fatigue analysis. Stress life fatigue is considered when the stress applied remains within the elastic range for the material selected and when the load cycles exceed 10,000. Strain life fatigue, on the other hand, finds application where load cycles exceed the elastic limit for the material with the development of a significant plastic component. The number of load cycles for such cases is usually below 10,000 cycles.

For stress life analysis, the fatigue data is represented in the form of the S-N Graph which is a measurement of the variation of the amplitude of the nominal stress over the cycles to failure. S-N data is usually recorded in the laboratory by subjecting the material under consideration to fully reversed stress cycles. In real world environment, cyclic stress is always a superimposition of alternating stress on mean stress developed due to the loading cycles. To include the effects of mean stress in a stress life analysis, several empirical relations like Goodman, Gerber, Soderberg, and Morrow have been developed over the years to define the variation of mean stress, with alternating stress, considering the yield and ultimate strengths. Figure 1 shows the graphs for the four types of mean stress compensation equations [1].

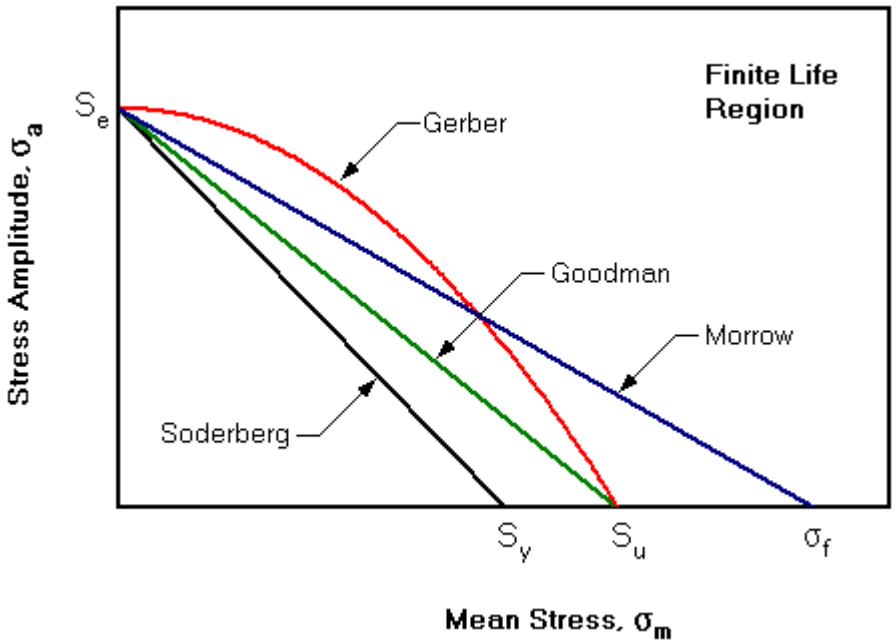

Figure 1. Mean stress correction equations [1]

Strain life fatigue analysis is applied to plastic strains usually developing in the notches with greater concentration of stress. The elastically stressed material with the small plastic zone causes the response of the material in that zone to be strain dependent. Fatigue response of materials have encompassed various elements of material study like metals, ceramics, composites, and polymers and have been applied to the fields of aerospace, mechanical and civil engineering, biomechanics, applied physics and mathematics. The mechanics of fatigue failure depends on the structure of the material under consideration. In metals with a crystalline structure, fatigue failure occurs when individual crystals slide along slip planes under the effect of external loading. This leads to the initiation of cracks that nucleate and propagate under subsequent loading eventually leading to fatigue failure [2]. In composites, progressive accumulation of damage in the form of fiber breakage, matrix cracking, transverse ply cracking, or delaminating eventually lead to fatigue failure [3]. Polymers, on the other hand, are more

prone to fatigue failure since accumulation of damage results in the development of repeated non elastic strain [4].Polymers, depending upon their ductility, and under the effect of fatigue loading, undergo cyclic softening. Cyclic softening of polymers occurs when the material offers less resistance to deformation for subsequent load cycles. The rate of cyclic softening is more in ductile polymers than amorphous or brittle polymers. Brittle polymers mostly remain stable in cyclic deformation and their fatigue response has been observed to be greatly affected by the strain amplitude [4]. Fatigue failure has been observed to vary under different environmental conditions. Corrosive environments and high temperature accentuate the process of fatigue failure.

The cyclic softening behavior of polymers is vital in the study of the fatigue response of soft tissues since they usually have been modeled as polymer or polymer composites. Two of the most important constituents of soft tissue, like arteries, are elastin and collagen. The mechanical properties of soft tissue depend greatly on the microstructure and arrangement of the collagen fibers [5]. Liao et.al [6] studied the stress softening behavior of the guinea pig oesophagus using a tri-axial test machine to determine the cause of softening in tissue to be viscoelasticity, or strain induced. Loss of stiffness due to viscoelasticity is a function of the time history of the load the tissue endures while the loss due to strain is dependent on the previous load cycles. It was observed that the stress softening in the tissue in both longitudinal and circumferential directions was due primarily to strain softening. The stress strain response of soft tissues is highly comparable to polymer composites since soft tissues have also been observed to cyclically soften and exhibit non linear behavior when subjected to continuous cyclic load.

1.2.2. Soft tissues: types and deformation details

Soft tissues can be classified into four different types [7]:

1. Epithelial
2. Connective
3. Muscular
4. Neural

The primary function of epithelial tissue is to provide structural support and protection to underlying tissue. It also performs certain specialized functions, however, depending upon its location. Epithelial tissue in the skin, for example, provide protection against mechanical injury, harmful chemicals and bacteria; on the inner lining of organs, like the intestine, it helps in nutrient absorption; on the kidneys, it helps in the excretion of harmful products; and on the glands, it secretes hormones, enzymes and lubricating fluids. Specialized sensory epithelial tissue, with nerve endings, is found in the skin, eyes, nose, ears and tongue. Epithelial tissue is made of closely packed cells with very little intercellular space and is usually arranged in one, or more, layers. Depending upon its structure, and function, epithelial tissue has been classified as squamous, simple cubodial, simple columnar, ciliated columnar, glandular, or stratified [7].

Neural and muscular tissue both have specialized functions. Neural tissue is made up of two kinds of cells, namely neurons and glial. Neurons consist of the cell body, or soma, axon and dendrite and are responsible for the conduction of sensory response in the form of impulse from various parts of the body to the brain. Glial cells, or neuroglia, are supporting cells found abundantly in the nervous system. Muscular cells are contracting filaments that move past each other to provide movement to different parts of the body. They are made of myofibrils containing scromeres composed of actin and myosin. Actin is a structural protein responsible for motility

and it also provides the scaffold for generation of muscular movement by myosin. Myosin is an ATP-dependent motor protein found mainly in muscle cells and is responsible for providing contractile motion to muscle cells involved in motility of any form. Individual muscle fibers are bound together in the form of bundles called fascicles, which in turn are grouped together to form muscle tissue. Muscles are broadly classified as skeletal, smooth, or cardiac. Skeletal muscles are also known as voluntary muscles and the movement of these muscles can be controlled by will while smooth and cardiac muscles present on organs and heart are involuntary muscles.

Connective tissues are abundant in ligaments, tendon, cartilages and blood vessels and are composed of cells scattered in an extracellular matrix. Connective tissue cells are of three types: Fibroblasts which secrete collagen in the extracellular matrix, adipocytes which are responsible for storing fat and mast cells, and macrophages and lymphocytes which perform immune functions. The extracellular matrix is composed of a ground substance consisting of water stabilized by glycosaminoglycans, proteoglycans, and glycoproteins. The fibers in the extracellular matrix are composed of collagen and elastin. Collagen provides tensile strength while elastin provides resilience to the connective tissue. The mechanical properties of soft tissues have been investigated in the literature and the load-deformation curve for all collagen based tissues has been found, in various studies, to be non-linear in nature. Figure 2 clearly identifies the different phases of the load deformation curve for soft tissue.

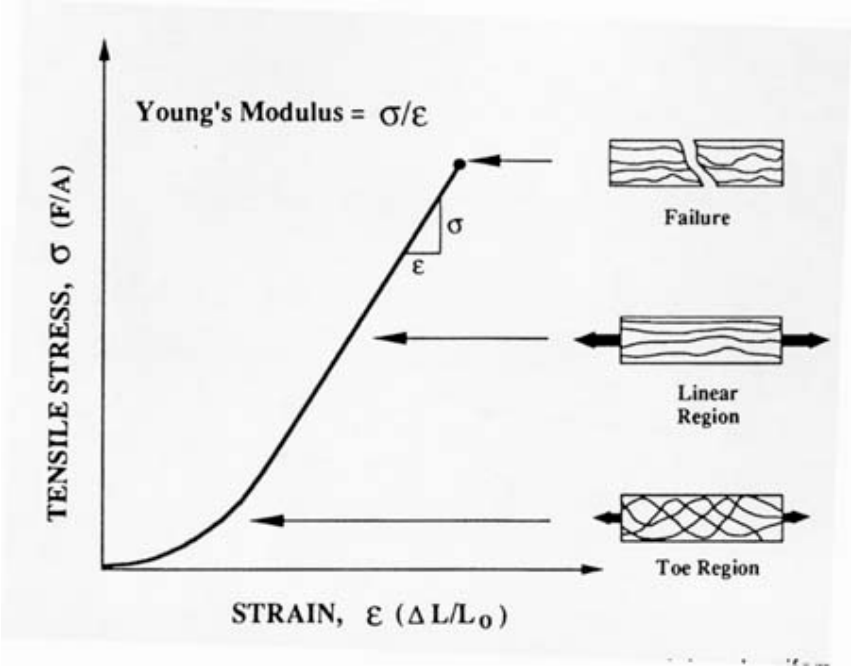

Figure 2. Stress vs strain response of soft tissue to loading showing the different phases [8]

The initial phase involves greater deformation for an applied force, followed by a phase where tissue deforms elastically. Immediately after the linear elastic phase, micro failure of collagen fibers is initiated resulting in sudden decrease in tensile force. Subsequent loading results in complete failure of tissue. Collagen fibers, when arranged in bundles, are flexed, and hence, under initial preconditioning load, the fibers extend easily under minimum force. Moreover, the arrangement of fibers is not linear. Hence, initially, non linear deformation is observed in soft tissues. After the fibers are straightened, stiffness increases with the increase in force linearly until the microfailure of individual collagen fibers occurs. Microfailure is a non-uniform process occurring at weak spots on random fibers rendering a nonlinear characteristic to the soft tissue at this stage. In the following phase, complete failure of fiber occurs resulting in a sudden drop of tensile force to zero. The linear elastic response of the fibers is described by the tensile modulus E. Deformation in soft tissues initially varies with time until it reaches

equilibrium. This equilibrium defined by the equilibrium modulus is a quantification of the quasi static behavior of the tissue which is governed by the tensile properties of the collagen fibers. The tensile equilibrium quantified by tensile modulus of soft tissue depends on the content and the arrangement of the collagen fibers within the tissue. An important characteristic of soft tissues is that they exhibit both elastic and viscous properties, and hence, are classified as viscoelastic materials. Elastic deformation occurs when the chemical bonds are not broken and the material returns to its initial form after the removal of force. Viscosity refers to the resistance offered to the movement between layers and viscous deformation involves the energy consumption. Viscoelastic responses can be defined by a time dependant response, a load history dependant response, or hyteresis. A time dependant response includes creep and stress relaxation. Creep is a phenomenon where deformation increases with time at a constant load, while with stress relaxation, stress decreases with time at a constant level of deformation. A history dependant response of viscoleastic materials develops different strain levels when stressed to the same stress level over the same time period following different paths. Hyteresis indicates the loss of internal energy during loading and consecutive unloading of viscoleastic materials due to the viscous component. Various mechanisms have been considered to be responsible for the viscoelastic behavior of soft tissues. For tissue with less water content, intermolecular motion between collagen, elastic and proteoglycan molecules under the application of force, viscous forces developed due to movement of the protein chains. Other complex intermolecular interactions have been considered, therefore, to contribute to the viscoelastic behavior. Whereas in tissue with higher water content, viscoelastic properties of soft tissue have been attributed to the viscous drag between protein molecules and water.

CHAPTER 2. LITERATURE REVIEW

2.1. Response of soft tissues under cyclic loading

Fatigue analysis of soft tissue is based on its response to cyclic load. Early studies on the fatigue properties of the Atherosclerotic plaque [9] and the sclera [10] have revealed stress softening of soft tissue under cyclic loading. There have been various attempts to characterize the fatigue behavior of soft tissues like tendons, articular cartilage, and heart valves. Based on experimental results researchers have derived various equations to illustrate the relation between the stress developed and number of cycles to failure. Initially, Wang [11] developed a linear model, as shown in equation (1), from his experimental results on the fatigue tests of wallaby tail tendon at a frequency of 1.1Hz.

$$S = 96.5 - 15.8\log(N) \quad (1)$$

He conducted his experiments over a range of frequencies and observed greater damage to the tendon at high frequencies. He also noticed a steady decrease in the 'stiffness ratio' defined as the fraction of stiffness over the initial stiffness of the specimen for samples stressed to different peak stress levels. The rate of decrease in stiffness was observed to be higher at higher peak stress levels indicating a greater extent of damage accumulation. Wang described the trend of stiffness variation in terms of the equation $s_r = 1 + at^3$, where $'s_r'$ is the stiffness ratio, 't' is-the time and 'a' is a parameter whose value is determined from the experimental results.

Later Schechtman and Bader [12] subjected 90 samples of human tendon to fatigue failure. All the specimens tested failed in a region between the clamped ends and each fiber that failed had a gradually tapered end. They formulated a linear model from their experimental results, as shown in equation (2)

$$S = 93.98 - 13.13\log(N) \quad (2)$$

For both the models, S is the normalized stress expressed as a percentage of ultimate tensile strength and N is the number of cycles. This model was found to be in close agreement to the linear model proposed by Wang except that fatigue failure in the animal tendon occurred faster than that in the human tendon. Schechtman *et.al* [12] observed higher fatigue damage accumulation at higher stress levels. At 40% of ultimate tensile, stress fatigue failure occurred at 8500 cycles, while for loading at 20% ultimate tensile, stress tendon failed after 300,000 cycles. In their studies, neither Wang, nor Schechtman, took into account the healing and remodeling process occurring in vivo and other factors like disease and age. Robert F. Ker *et.al* [13] compared the fatigue quality of different tendons from the Wallaby tail and hind limb. They observed that low stressed tendons have a lower resistance to stress and that they fail faster than higher stressed tendons in the mammalian body. Weightman [14] studied the fatigue response of cartilage by applying cyclic tensile load to the cartilage sample in the direction of the collagen fiber, and derived expressions (3) and (4) in terms of fracture stress (S_f), age of the joint (a), tensile stress applied (S) and the number of cycles to failure (N)

$$S_f = 25.4 - 0.15a \quad (3)$$

$$S = S_f - 1.65\log N \quad (4)$$

From his results, he concluded that cartilages are prone to fatigue, higher fatigue is observed at higher stress levels, and that the fatigue life of cartilages decreases with age. The age of the cartilage was found to be more crucial in determining the process and time of fatigue failure compared to the content of collagen and proteoglycan. Weightman observed that the highest peak contact pressure at the femoral head of the order $5MN/m^2$, combined with the maximum compressive stress of $8MN/m^2$, can lead to fatigue failure in cartilages weakened by age.

Bellucci and Seedhom [15] studied the mechanical behavior of articular cartilage under tensile cyclic load imposed on the cartilage due to walking. Based on their experimental results, they concluded that the range of cycles to failure for the cartilage is 2 to 1.5 million cycles. One of the most interesting observations of this study was the zonal variation in fatigue properties within the cartilage. The superficial and deep layers were found to possess more fatigue resistance compared to the middle layer when stressed both in the perpendicular, as well as parallel, to the orientation of the collagen fibers. This observation suggested that the fibers in the middle layer are more loosely and randomly oriented while those in the surface, or in the deep layers, are closer and packed more orderly, rendering better mechanical properties. It was also observed that the fatigue resistance of fibers in the direction parallel to the orientation of the collagen fibers were much higher compared to the perpendicular direction. All the aforementioned experimental procedures indicated stress softening in the material with an increase in the number of cycles.

Broom [16] studied the effect of accelerated cyclic loading on porcine and bovine heart valves at a frequency of 35Hz. From his results, he concluded that the tissue compliance is reduced and the collagen fiber structure is altered due to the cyclic loading. He suggested that the cyclic, or repeated, nature of loading was a more crucial factor affecting the process of cavitation and matrix removal leading to fatigue failure, when compared the levels of physiological stress. In his study, however, external factors like in-vivo biological conditions under which the heart valve operates, or the conditions under which the heart valves are preserved and their affect on the structure and composition of the valves when tested, were not considered.

Wells and Sacks [17] conducted tests at a frequency of 15Hz where the samples of bioprosthetic valves were cycled up to 2×10^8 times to analyze the effects of fixation pressure.

They concluded that though collagen fibers may remain chemically unaltered when subjected to long term cycling, they may undergo few conformational changes during the period of loading. Yokobori [18] noticed reduced ultimate strength of canine thoracic artery after they were subjected to 20000 cycles of internal pressure of varying amplitude. On the basis of his experimental data, he concluded that an artery subjected to pulsatile pressure of varying amplitude endures more mechanical damage than one subjected to constant amplitude pulsatile pressure. The decrease in fracture strength of tissue under varying amplitude pulsatile load was attributed to plastic elongation of collagen fibers. McCord [9] also noticed a reduction in stiffness of human arteries containing plaque when subjected to cyclic loading. Gilpin [19] also observed stress softening of porcine coronary artery when the samples were loaded in cycles under different loading conditions until failure. She obtained an S-N curve to characterize the fatigue behavior of the porcine coronary artery. The histology samples for the experiment showed the development of circumferential tears in the tunica media layer of the artery indicating fatigue damage. Thus, any kind of soft tissue has been observed to exhibit a stress softening when subjected to cyclic loading over a period of time.

2.2. Arterial structure and mechanics

The mechanical properties of an artery are dependent on the structure, composition and location of the artery within the body. All arteries are three layered structures consisting of Tunica Adventitia, Tunica Media and Tunica Intima, as shown in Figure 3.

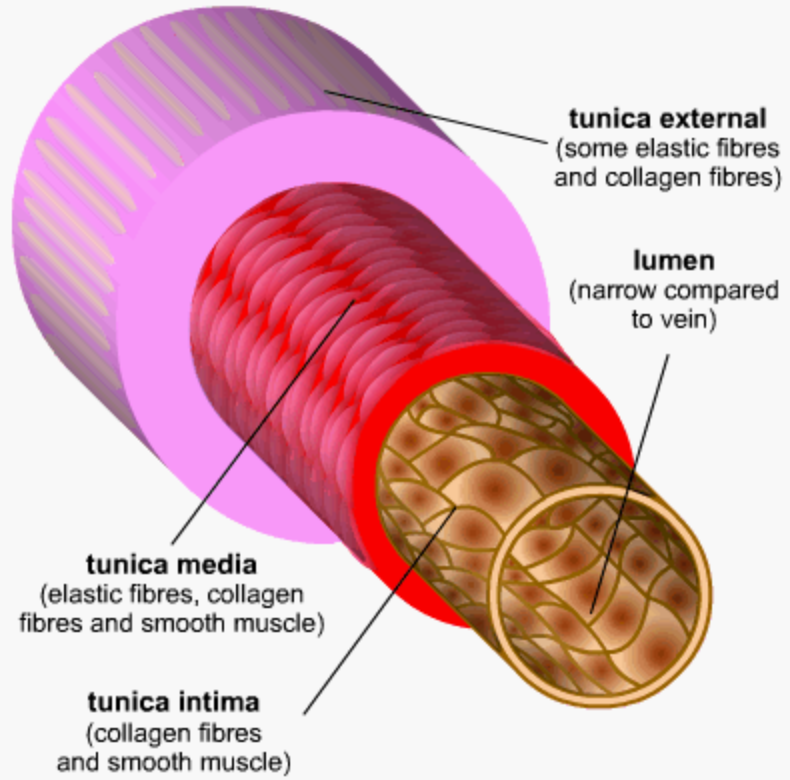

Figure 3. Internal structure of artery showing the three different tissue layers [19]

Tunica Adventitia is the outer layer of the artery consisting mainly of connective tissue with collagen and elastin fibers which allow the arteries to stretch yet prevent over expansion and tear due to the intraluminal pressure. The collagen fibers within the tunica adventitia are loosely woven and help anchor the artery to surrounding structures. The structure of adventitia varies for different arteries and may change under different mechanical conditions [21]. In the coronary arteries of young animals, the collagen and elastin fibers remain distinct, but with age the adventitial layer becomes thin, due to intimal thickening. In renal arteries, however, the adventitia remains distinct inspite of intimal thickening.

Tunica Media is the middle layer of the artery consisting mainly of smooth muscle cells and sheets of elastin fibers. Smooth muscle cells help in movement of the arterial wall while the elastin fibers allow the artery to stretch and recoil. The detailed structure of the media has been

studied using thin micro structural sections and ultra structural preparation. Studies have revealed that the media is a composite structure made of subunits arranged to forms layers within the media [22]. Each subunit consists of a group or fascicles of smooth muscle cells bound together by continuous intercellular and pericellular basal lamina and a fine network of collagen fibers .The smooth muscle cells within the unit is attached to the surrounding elastin fibers by firm linear connections. Independent bundles of coarser collagen fibers are also present in the media, but they are not attached to the elastin fibers. The relative collagen and elastin content within the artery is subjective to various factors like the distance of the artery from the heart, growth rate of supplied organs, flow profile and velocity of cardiac cycle and age.

Tunica intima is the inner most layer of the artery and is composed of elastic membrane lining and smooth endothelium. This layer remains in contact with the blood and the endothelium serves as a smooth lining to reduce friction. The endothelium cells are polygonal, oval, or fusiform with distinct oval, or round, nuclei. The subendothelial layer consists of branched cells within the connective tissue matrix. The elastic layer consists of a network of elastic fibers arranged in the longitudinal directions. This layer is the principal component of the tunica intima.

Biologically, the structure of the artery varies to maintain an optimal tensile and shear stress within the artery. An example of such adaption would be the morphological changes in the ascending aorta and pulmory trunk at birth and thereafter. At birth, the blood pressure in the aorta and the pulmonary trunk is almost the same and which is equal to half of that in a normal adult.After birth, however, the aortic pressure doubles while the pressure in the pulmonary trunk falls to half of what its value was at birth. Due to increased aortic pressure at the post natal stage, though the radius and length of the vessels remain the same, the tunica media of the aortic

wall grows faster than that of the pulmonary trunk. The rate of matrix fiber accumulation within the vessel wall depends on the wall tension, but the rate of increase in the number of smooth muscle cells remains the same in both segments. Due to the difference in the rate of production of matrix per cell in different arterial segments,the arterial wall architecture also becomes distinct. Under the effect of increased intraluminal pressure, therefore, each transmural layer of the media thickens to increase the overall cross-sectional area. The number of layers of the media, however, remains the same.

The arterial adaptions for maintaining optimal shear stress include intimal thickening, and an increase, in the radius of the artery. An increase in the wall shear stress over the normal level of 15dyn/cm^2 results in a gradual increase in the arterial radius to accommodate for the increase in wall stress. A decrease below the normal level of smooth muscle cell proliferation takes place in the intima thereby thickening it and reducing the size of the lumen. Reduced lumen size results in increased wall shear stress. If the flow velocity is not increased sufficiently after intimal wall thickening, the process may finally lead to pathological stenosis, or disappearance, of the lumen as a whole due to excessive thickening of the intima.

The structure and composition of the individual layers in the artery play a crucial role in the mechanical response of the artery. The tissue components can be classified as active and passive. The most important passive components are collagen, elastin and smooth muscle cells. Glycosaminoglycan is a rich ground substance and is one of the active components that can participate in altering arterial wall mechanics by altering its ion and water binding potential [23]. The circumferential properties of the arteries are of utmost importance since the arterial motion predominantly occurs in the circumferential direction due to pulsatile blood flow generated by the cardiac pulse. Mechanical properties and structure of elastin and collagen fibers determine

the circumferential response of arteries. Elastin is a fibrous protien in the form of long, independent polymeric chains and exhibits linear, or non linear, elastic properties. For a linear stress strain curve, the Young's Modulus (E) is defined as a means of quantitative measure of stiffness, E= $\frac{\sigma}{\epsilon}$. For a non linear stress strain curve the stiffness is a measure of the incremental Young's Modulus which is defined by the slope of the stress strain curve at designated points $E_{inc} = \frac{\Delta\sigma}{\Delta\epsilon}$. Collagen is also a fibrous protein with a more complex helical structure of three protein chains wound about the vertical axis to form the helix as shown in Figure 4. These individual protein chains are connected with numerous interchain links which contribute to the high mechanical stiffness of collagen fibers. These interchain links are two aldimine bonds which provide stability to the protein chains and hence reduce movement or deformation between chains, hence rendering stiffness to collagen fibers [24]

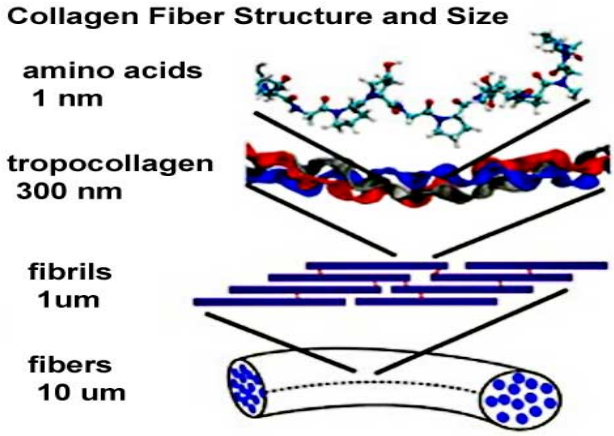

Figure 4. Structure and constituents of collagen fibers and their size [24]

In vivo increased arterial stiffness was observed with increased tissue extension. Various studies have been conducted thereafter to determine the morphological changes in the collagen

and elastin fibers that lead to increased arterial stiffness with tissue extension. Reuterwall [25] observed the collagen fibers to be curled and loose in retracted arteries, but extended and taut in stretched arteries. Roach and Burton [26] tried to analyze the contributions of elastin and collagen separately in the overall mechanical properties of the artery. They used crude trypsin and formic acid to degrade elastin and collagen fibers, respectively, in the tissue sample. Based on their results they concluded that elastin supports load in circumferential direction at a lower level of tissue distention, but at higher levels, equivalent to physiological collagen, it acts as the primary load bearing fiber. Wolinksy and Glagov [27] examined histological samples of rabbit aorta subjected to pressure ranging from 5 to 200 mm of Hg. At low pressures they observed that both the elastin fibers and the collagen fibers, arranged circumferentially in the media, remain retracted and loose. At pressure levels equivalent to physiological pressure, both the collagen and elastin fibers in the media remain taut, but those in the adventitia were randomly oriented. The experimental observations suggested that elastin provides the stiffness to the artery at lower pressure levels while at physiological pressure both the elastin and collagen fibers provide stiffness. Peterson *et.al* [28] devised a measure of the stiffness of arteries known as the 'Pressure elastic modulus' E_p similar to Young's modulus. Pressure elastic modulus can be used to measure the arterial stiffness in vivo $E_p = \frac{\Delta P \times r}{\Delta r}$, where Δ P is the pressure oscillation occurring in each cardiac cycle, Δ r is the oscillation in arterial radius occurring due to pressure oscillations, and r is the mean radius of the artery. It was observed that the E_p increases with increased distance from the heart for all blood vessels. The circumferential strain for a cylindrical section of the artery is expressed as , $\epsilon_\Theta = \frac{\Delta r}{r_0}$ and circumferential stress is

expressed as $\sigma_{\square} = P_T \times \frac{r_i}{h}$, where r_0 the radius of unpressurized vessel is, P_T is the transmural pressure, r_i is the internal radius of the artery and h is the arterial wall thickness. Various models have also been developed to elucidate the contributions of elastin and collagen fibers to the stiffness of arteries. Initially, two parallel springs were used to represent elastin and collagen fibers. This model overlooked the increased contribution of stiffness of collagen fibers at larger strain levels. Wiederhielm [29] developed another model with a compliant spring connected to a stiff spring by means of a hook which is only engaged at high strains. Dashpots have also been included in this mode to account for the viscous behavior of blood vessels.

2.3. Fatigue analysis in finite element (FE)

Fatigue analysis in FE helps predict the life of a material, or structure, when subjected to cyclic loading over a period of time. Use of FE analysis helps locate the exact areas that accumulate the maximum amount of stress, or undergo highest deformation under cyclic loading. ANSYS Workbench 2.0 is FE software which defines a special fatigue tool for fatigue analysis of structures, or materials. The alternating stress versus life cycle graph is used to define the fatigue material properties for stress life data option. Four different kinds of fatigue loading that can be applied are: 1) constant amplitude proportional loading, 2) non constant amplitude proportional loading, 3) constant amplitude non proportional loading, and 4) non constant amplitude non proportional loading. In constant amplitude proportional loading, the amplitude of load remains constant and, since the load is proportional; the principal stress axes do not change over time. Hence, a single set of FE stress results, along with the loading ratio, would be required to compute the alternating and mean stress levels.

In non constant proportional loading, instead of single amplitude, the loading ratio keeps changing over time, as shown in Figure 6. Though the critical areas susceptible to fatigue damage can be ascertained by looking at a single state of FE stress results, the fatigue load causing the maximum damage cannot be identified. Cycle counting, using Rainflow matrix, and damage accumulation, using Miner's rule, are applied to determine the total fatigue damage, as well as which cycle caused the damage.

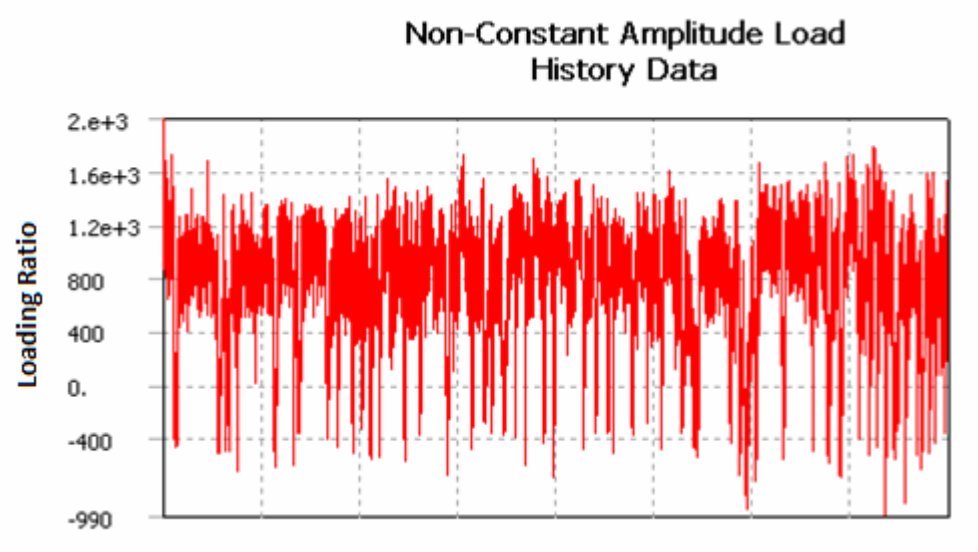

Figure 5. Non constant amplitude loading history data [30]

Loading is identified as non proportional when two or more distinct load types like bending and torsion are applied, when a static load superimposes an alternating load, or when the direction of load application keeps changing. Since the loading is non proportional, the critical fatigue location occurs at a spatial location. For all load types, the mean stress correction is applied to account for the mean stress when the loading is not fully reversed and where mean stress is zero. Goodman, Gerber, Soderberg are the empirical methods for accounting for mean stress [30]. Experimental data for different r-ratios, if used, are interpolated during analysis to

directly account for the mean stress levels. For experimental data calculated at different r-ratios, or mean stress, the empirical mean stress correction theories mentioned earlier are not accurate enough.

2.4. Literature survey on fatigue analysis of arteries

The present study emphasizes analyzing the fatigue response of human coronary arteries and has four specific aims:

- to compare the change in fatigue life and extent of stress accumulation of normal and hypertensive arteries;
- to analyze the effect of age on the change in fatigue life of arteries;
- to analyze the effect of the undulation of arteries on fatigue response and analyze the change in fatigue properties of arteries due to different amplitudes of undulation and
- compare the fatigue response of artery surrounded by tissue material to those without the tissue with the primary intention to identify the effects of surrounding tissue material on the fatigue properties of arteries.

The issue of hypertension and its effect on arteries have been addressed by researchers from different perspectives. Armentano *et.al* [31] studied the effects of hypertension on the viscoelasticty of human carotid and femoral arteries and observed a reduction in compliance and distensiblity, as well as an increase in wall viscosity for both kinds of arteries due to hypertension. They observed a reduced femoral pulse diameter in hypertensive patients, but the carotid artery pulse diameter remained the same for hypertensive and normotensive patients. Their findings suggested alterations in the geometric properties of the femoral artery due to hypertension which caused intrinsic dialation and subsequent loss of pulsatile distension.

Moreover, they also observed that the intrinsic elastic properties of the carotid artery were not altered under hypertension, unlike that in the femoral arteries where reduced compliance, and distensibility, was observed at hypertensive conditions. Sharma and Hollis [32] studied the rheological properties of rabbit aortas under normal and hypertensive conditions for different constant strain values. . Hu *et.al* [33] also observed a similar increase in stiffness of the porcine basilar artery under hypertension. Lichtenstei *et.al* [34] studied the static and dynamic mechanical properties of carotid arteries from normotensive and hypertensive rats. They observed reduced compliance and distensibility in the arterial wall of hypertensive rats under static conditions. Under dynamic loading conditions, the carotid wall compliance and distensibility were almost similar for normotensive and hypertensive rats.

Intengan and Schiffri [35] studied the factors leading to reduced compliance and distensibility in hypertensive arteries. They observed change in arterial stiffness due to alteration in collagen elastin, or smooth muscle content in the wall, to be one of the main causes of reduced compliance for hypertensive arteries. Extracellular matter, like proteoglycans, was also identified to alter vascular thickness. They concluded that abnormalities in the endothelium, adhesion molecules, and extracellular matrix (ECM) in the arterial wall, alter the structural mechanical and functional properties of arteries under hypertensive conditions. Though there have been few studies on the changes in the structural and mechanical properties of arteries under hypertension, there is no significant study on the effect that these structural and mechanical changes in the artery have on fatigue properties, or the extent of damage accumulation in the arteries.

The mechanical properties and wall structure of arteries have also been studied over different age groups to identify any morphological changes in the artery with ageing. Ozolanta

et.al [36] carried out experiments on the proximal and distal parts of the coronary artery for ages 1 day to 80 years. They observed an increase in wall thickness of the artery as age increased, but the process of collagen or the addition of ECM, was noticed to be non uniform at different layers for different age groups. The stretch ratio and the tangential modulus in the circumferential direction were also observed to change for different age groups and gender. Van der Heijden-Spek *et.al* [37] studied the effects of variation in compliance and distensibility of arteries by age for different vascular regions and genders. Based on their results, they concluded that distensibility of the aorta, for both genders, decreased with age, whereas no relation could be observed between the compliance and distensibility of the brachial artery of either men or women. Instead of a decrease in distensibility with age, in women, it was observed, however, that distensibility of the brachial artery increased with age. Cameron *et.al* [38] studied the changes in the mechanical properties of arteries with age for normal and type 2 diabetic patients. They observed age related deterioration in both elastic and muscular arteries for normal and diabetic patients, but the extent of deterioration for diabetic patients was greater. Increased age related damage of arteries in diabetic patients could be attributed to high blood pressure, and eventually a higher pulse wave velocity, in the arteries due to diabetes. Diabetic arteries were observed, therefore, to stiffen earlier and at an accelerated rate when compared to normal arteries. Reddy *et.al* [39] compared the aortic input impedance spectra, pulse wave velocity and augmentation index of adult and older mice to understand the difference in the stiffening of arteries in mice. Characteristic impedance was observed to be 57% higher in older mice and the pulse pressure and augmentation index were also observed to be higher in the older mice. Thus, the effect of age on arteries has been studied under various aspects, but there has been little investigation into the variation of fatigue properties of arteries with age. This study emphasized

the changes in mechanical properties of arteries with age and their effect on the fatigue response of arteries.

This FE study analyzed the effect of arterial undulation on the fatigue response and the extent of stress accumulation that it caused. Arteries buckle when they lose their stability due to reduced axial strain, hypertensive blood pressure and also ageing, or weakening of the wall. Han [40] developed a biomechanical model to elucidate the process of arterial undulation. He developed equations to relate the critical pressure, at which undulation of arteries occurs, to arterial length, radius, wall thickness and axial stretch. From his results, he concluded that arteries may buckle due to high intraluminal pressure. He also observed that the critical undulation pressure was proportional to the stretch ratio and Young's modulus of the artery. He also suggested that if the axial tension in the arteries drops below the physiological level, arteries will tend to buckle. In another model that Han [41] developed, he considered the artery to be non linear and thick walled and included the effects of residual stress, as well. He observed that the residual stress within the artery significantly affected the critical pressure. Although there have been previous studies in determining the causes and the critical pressure at which undulation of arteries set in, no literature was found on the effect of this undulation on the mechanical response of arteries. FE simulations are used to understand the effect of undulation on the shear stress distribution and on the fatigue life of arteries.

The FE model developed for this study also compared the effect of surrounding tissue material on the fatigue response of arteries. This was done to take into consideration the effect of in-vivo circumferential pressure on the arteries, due to the stiffness of the surrounding tissue. Zhang and Greenleaf [42] analyzed the effect of tissue mimicking gelatin on arterial response. A short pulse wave was generated within the arterial wall which was measured using a scanning

technique. The response of the artery, with and without the gelatin, was analyzed by measuring the wave velocity. They concluded that tissue mimicking gelatin stiffens the artery. M. B Restrepo [43] studied the effect of surrounding tissue material on Young's modulus of the arteries by conducting tests on artery samples surrounded by gelatin. He observed stoical differences between Young's modulus of arteries with and without the surrounding gelatin at 10, 80 and 100 mm of Hg. He suggested that undulation of arteries, without the surrounding gelatin, might lead to variation in Young's modulus at high pressure levels. In comparing the Young's modulus to pressure relationships for both situations, he suggested that gelatin does not play a role in altering the response of the arterial wall at different internal pressure levels. This paper attempts to compare the fatigue response of arteries, with and without the surrounding tissue, and to analyze the effect stiffness of the surrounding tissue has on the fatigue life of arteries.

CHAPTER 3. FATIGUE FINITE ELEMENT ANALYSIS METHODOLOGY

3.1. Finite element modeling: structure, properties and meshing

Three different FE models were developed for the purpose of this research. The artery was modeled as a hollow cylindrical structure for the purpose of comparison between normotensive and hypertensive arteries. The arterial structure was kept simple for this investigation since the intraluminal blood pressure and mechanical properties of normal and hypertensive arteries play a crucial role in determining the variation in fatigue response due to hypertension. It was assumed that the artery had a uniform circular cross-section with an external diameter of 3.51 mm and an internal diameter of 2.15 mm [36]. The dimensions selected for the purpose of developing the FE model were those of a human coronary artery. The external diameter and the thickness of the FE model of the artery were altered according to those measured at different ages, in order to investigate the effect of age on fatigue properties of the artery. The different dimensions selected for different age groups were the same as for the human coronary artery. Five different age groups were selected for the purpose of the comparison. Table 1 illustrates the external diameter and thickness of the artery for each selected group.

Table 1. Thickness and external diameter of arteries for different age groups used in the FE simulation

Group	Age	External Diameter (mm)	Thickness (mm)
1	0-1	1.26	0.2
2	1-7	1.9	0.4
3	8-19	2.28	0.43
4	20-39	3.42	0.75
5	40-59	3.43	0.69

This study also emphasized the effects of arterial undulation on fatigue life. For the purpose of this study the basic FE model of the artery was altered to provide amplitude of undulation to the structure. Four amplitudes of undulation, of the order 0.4mm, 0.8mm, 1.2mm and 1.6mm, have been selected for this purpose. The extent of undulation, or undulation, is determined by artery location, intraluminal blood pressure and various other intrinsic factors. The four amplitudes of undulation were also considered when the FE model of the artery was created with a circular cross-section of tissue around it. The external diameter of the tissue material was assumed to be 5mm while the internal diameter was considered to be equal to the external diameter of the artery, which was 3.51mm [36]. The tissue material selected to be completely bonded to the artery for the purpose of the analysis. The model represented a small section of a long artery and was referred to as the Representative Volume Element (RVE). The continuity of the artery along the length was accounted for in the analysis by the implementation of Periodic Boundary Condition. Figures 8, 9 and 10 show the different FE models created for the purpose of this study.

Meshing was the application used to divide the model into FEs consisting of nodes. The element type used for this analysis was Hex20 which was internally chosen by Ansys. A global meshing tool was utilized to create a symmetric mesh for the model. Mapped mesh was created on the circular cross-section of the artery with tetrahedral elements. This mesh was swept along the length of the model to divide it into symmetric hexagonal elements. The element size for this purpose was 3×10^{-4} m which insured a small enough mesh for proper representation of the stress accumulation over the artery model. The smoothing function, which attempts to improve the element quality by moving the location of the nodes with respect to other nodes on surrounding elements, was set to medium. The transition rate that controlled the rate at which the

adjacent elements grew was kept slow to ensure a smooth element transition. The span angle center, which defines the angle that elements span at a curvature, was kept between 91 to 60 degrees in order to avoid too fine of mesh at the curvatures which could lead to incomplete solution of finite element equations in ANSYS resulting in erroneous results. The element quality, which is defined as the ratio of the volume of the element to the edge length, ranged from 0.9926 to 0.1368. A value of 1 indicates a perfect square, or a cube, while that of 0 indicates negative volume. The aspect ratio for the mesh varies from 9.4691 to 1.0438. The Jacobian ratio gives a measure of the reliability of the mapping between element space and real space. A higher ratio indicates unreliable mesh. The Jacobian ratio for this model ranged from 1.5849 to 1.073. Quadrilateral element would have a Jacobian ratio of 1 if the opposite edges were equal and parallel to each other. The element warping factor is a measure of the extent of warping in the element. A higher factor indicates mesh generation flaw. The warping factor for the mesh generated for the model of the artery ranged from 2.468×10^{-6} to 0.1268 which is low. The parallel deviation is a measure of the extent to which the parallelism of two opposite edges of the element deviate. The mesh created for the model ranged from 20.386 to 5.3565. The maximum corner angle for the element ranged from 163.54 to 93.86. The skewness of the elements varied from 0.817 to 6.5864. Skewness is the measure of how close the equiangular structure is to the triangular or quadrilateral elements. Two separate models were created: 1) one with the tissue material around the artery and 2) the other without tissue around the artery. There were 23,519 nodes and 4,234 elements created for the model of the artery without surrounding tissue, while in the model of the artery with surrounding, 60,825 nodes and 10,950 elements were created.

3.2. Micromechanics of the finite element model

Micromechanics is the branch of engineering which deals with constricting the concentration of any kind of analysis to the level of microns. It involves considering small unit cells which part of a larger continuum thereby, eliminating the requirement of considering the effects of forces on the volume, or surface. The main aim of micromechanics is to bring the order of homogeneity into structural, or material, inhomogeniety to make the study of complex geometries and heterogeneous materials easier. In a micromechanical study, the characteristic length of a micromechanical unit is smaller than the actual body, but larger than the size of the molecule, and depends on the characteristic size of the heterogeneities. The molecular effects are not considered in micromechanics.

The concept of micromechanics was applied in this FE analysis to determine the effect of intraluminal pressure within a small continuous section of the artery away from the surface. The model of the artery was divided into smaller units, or, and, instead of solving the problem for the entire body, equations were formulated for each FE within the body and then combined to obtain the solution of the whole body. Each FE model was made of a number of nodes at which the displacements and stresses were calculated. The FE type was selected to model, most closely, the actual physical behavior of the body. A displacement function was created for each FE and, using the stress/strain properties, the behavior of each node in an element was computed. Each equation for every node was included in the equation set which was solved to obtain the solution for the entire body.

Two different approaches were applied in the study of the micromechanical FE model. The force or flexibility method uses internal forces as the unknown quantities in the problem

while the displacement, or stiffness, method assumes the displacement at the nodes as the unknown in the problem.

3.3. Fatigue analysis methodology in ANSYS

Fatigue analysis of the unit cell is completed using FE software ANSYS [44]. The fatigue tool within ANSYS Workbench requires the definition of fatigue material properties in terms of alternating stress versus life graph of the S-N graph. The S-N curve, obtained experimentally for the porcine coronary artery, is utilized as material characterization input for the fatigue analysis of the artery [45]. The material is subjected to high cycle fatigue loading since the expected number of load cycles during the lifetime is more than 1000. For high cycle fatigue, the material is subjected to lower loads for a longer period of time and, hence, the stress developed is usually much smaller than the yield stress. The material usually undergoes elastic deformation under such conditions. In high cycle fatigue a stress-life approach is adopted. It is based on the empirical S-N curve and modified by factors like mean stress correction. Four different types of mean stress correction can be selected in ANSYS to account for the mean stress. The first type of correction is the one where the mean stress is accounted for directly through interpolation from the experimental data provided. This is done when an S-N graph is provided for one, or more, R-ratios, or means stress levels. If the R-ratio, or the mean stress, for a particular S-N graph is not available experimentally, empirical options like the Gerber, Goodman or the Soderberg theories are applied to account for the mean stress in the fatigue analysis. The Goodman theory is a good option when conducting fatigue analysis of brittle material while Gerber theory applies well to ductile materials. Both the Goodman and Soderberg theories ignore negative or compressive mean stress that might develop, since compressive stress retards the process of fatigue failure

and, hence, are considered more conservative in their approach. The following equations represent the different theories of mean stress correction for stress life fatigue analysis:

$$\frac{\sigma_{Alternating}}{S_{Endurance\_limit}} + \frac{\sigma_{Mean}}{S_{Yeild\_strength}} = 1 \quad Soderberg\ Equation \tag{5}$$

$$\frac{\sigma_{Alternating}}{S_{Endurance\_limit}} + \frac{\sigma_{Mean}}{S_{Ultimate\_strength}} = 1 \quad Goodman\ Equation \tag{6}$$

$$\frac{\sigma_{Alternating}}{S_{Endurance\_limit}} + (\frac{\sigma_{Mean}}{S_{Ultimate_{strength}}})^2 = 1 \quad Gerber\ Equation \tag{7}$$

Fatigue design and analysis involves the consideration of the following aspects:

- Loading
- Stress analysis
- Material properties
- Rainflow cycle counting
- Alternating stress analysis
- Palmgren –Miner rule
- Fatigue analysis in this study

3.3.1. Loading

The nature of load is one of the crucial factors that determine the fatigue response of the artery. The intraluminal blood pressure varies between the systolic and diastolic pressure and, hence, is considered to be a pulsatile load with constant amplitude and proportional in nature. The loading type is proportional as the first cycle of load variation is repeated throughout the lifetime. The loading ratio, or R-ratio = P_{MAX}/P_{MIN} , which in this study was the ratio between

the systolic and the diastolic human blood pressure, is 1.8. For the purpose of this study none of the empirical mean correction theories were applied since the alternating stress versus life cycle graph was assumed for a specific R-ratio. The fatigue strength reduction factor is applied to account for the real environmental conditions that may be harsher than controlled laboratory environment. The alternating stress is divided by the fatigue strength reduction factor to account for the changes in the actual environment. ANSYS fatigue module requires the specification of fatigue strength factor. The fatigue strength factor for the coronary artery was not available in the literature and, hence, was assumed to be 1 for the simulation completed in this study. The actual environment under which the artery existed was, therefore, assumed to be the same as the laboratory environment under which the cyclic tests on the artery tissue were completed.

3.3.2. Stress analysis

The geometry and boundary conditions applied to the structure under investigation plays an important role in determining the stress development and, hence, the fatigue life of the body. FE techniques are utilized to locate the areas of high stress which are susceptible to greater fatigue damage accumulation.

3.3.3. Material properties

Proper definition of material properties of the body is essential since fatigue is a localized phenomenon dependant on the extent of stress accumulation and the amount of strain developed. The stress strain relationship is unique for a particular material and, hence, in the analysis of fatigue behavior of a structure, proper definition of the material properties is pivotal to the study. The material properties obtained from a small specimen subjected to uni-axial tests in the

laboratory can, therefore, be effectively utilized for analyzing the fatigue behavior of a different structure, but made of the same material.

Fatigue analysis in ANSYS involves three aspects of calculations:

- Cycle counting using the Rainflow counting technique;
- Alternating stress calculation for fatigue life prediction; and
- Cumulative damage accumulation using Palmgren –Miner rule.

3.3.4. Rainflow cycle counting

Random stress fluctuations occur when structures are subjected to cyclic loading. Several stress peaks appear over time, due to these fluctuations, and, thus, it becomes difficult to calculate the number of cycles that the structure absorbs during the entire length of cyclic loading. The Rainflow counting technique is used to overcome this difficulty and calculate the number of stress cycles the structure absorbs based on an algorithm [46]. For the purpose of the counting, if the positive maximum is considered a peak, the drop in stress to the lowest value is considered the valley. The algorithm can be explained in the following steps:

1. Move to next available peak or valley. If none exists move to step 6.
2. X is the previous peak or valley and Y is the present peak, or valley, recorded
3. Compare the values of X and Y.
    - If $X<Y$, go to step 1
    - If $X\geq Y$, go to step 4
4. If Y contains the starting point, go to step 5; and if the starting point is on X, count Y as one cycle. Discard the peak and valley of Y and go to step 2.

5. If Y contains the starting point count, it as a half cycle and move the starting point to the next peak.
6. Each range not counted previously is counted as a half cycle

For the stress fluctuation graph shown in Figure 7, counting starts at valley A, moves to B and then stops since the range of the next valley C is greater than that of A. Hence, AB is half the cycle of range 3. Counting resumes at peak B and moves to C and then again stops since the range of the next peak D is higher than B. BC is a gain and is counted as a half cycle of range 4. Next, the starting point moves to C and continues until F. Since neither D, E nor F is the starting point, EF is considered as one whole cycle and removed from the plot. CD, DG, GH, HI are all half cycles. The total cycle counts for the fluctuating stress diagram can be summarized as follows:

Table 2. Rainflow cycle counting

Range (units)	**Cycle counts**	**Events**
10	0	
9	0.5	DG
8	1	CD, GH
7	0	
6	0.5	HI
5	0	
4	1.5	BC,EF
3	0.5	AB
2	0	
1	0	

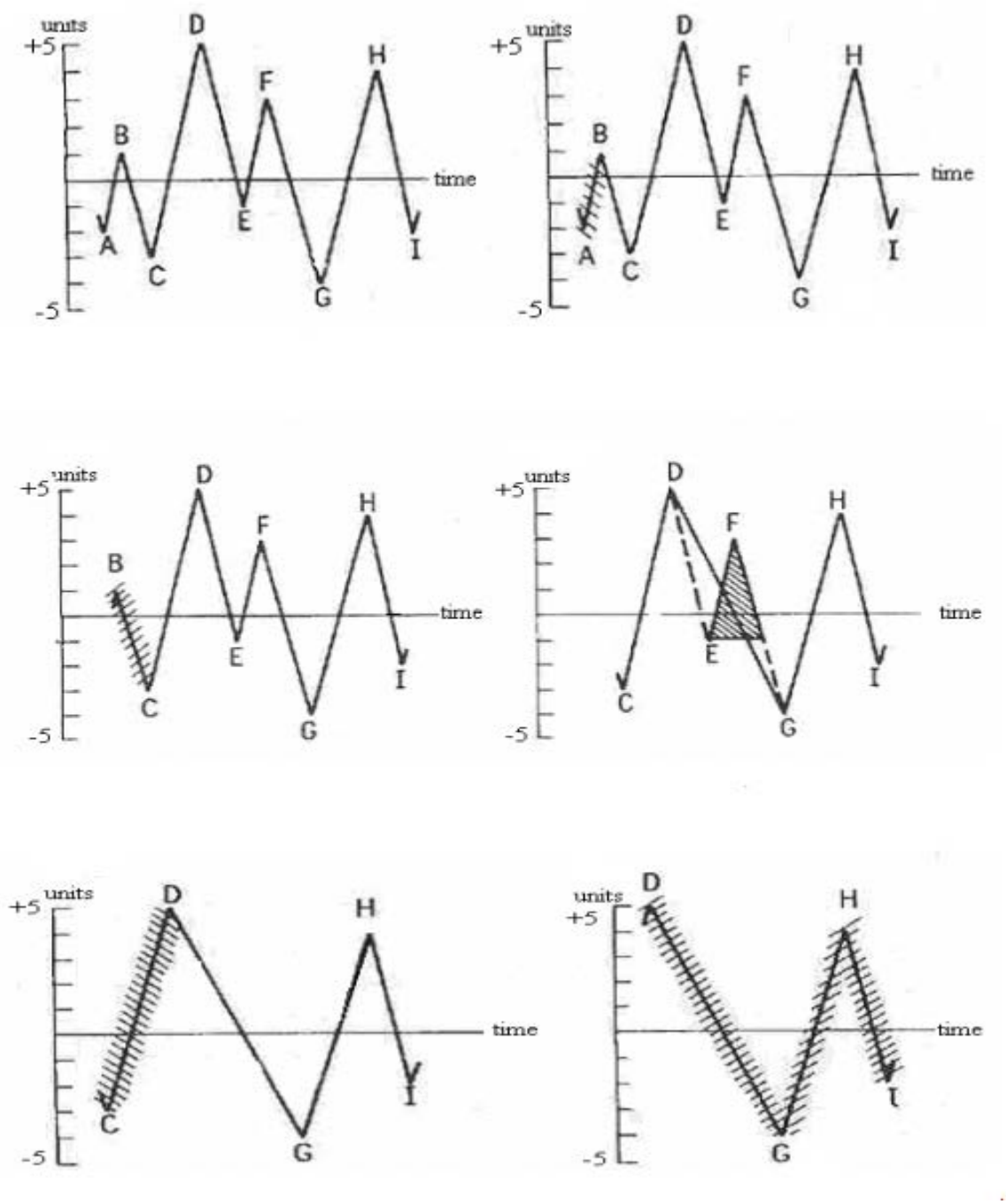

Figure 6. Rainflow cycle counting graphical description [46]

3.3.5. Alternating stress calculation

In cyclic loading for constant amplitude and proportional loading, the loading fluctuates between two load pairs, resulting in the development of alternating stress.

The maximum alternating shear stress is computed using equation 8

$$\{\sigma_{ij}\} = \sigma_i + \sigma_j \tag{8}$$

where σ_i is the stress vector corresponding to load vector l_i and σ_j is the stress vector corresponding to load vector l_j. For the loading pair producing the maximum alternating shear stress at a node location, the principal stresses $\sigma_1, \sigma_2, \sigma_3$ are recorded. For constant amplitude proportional loading, only one load pair is repeated for n number of cycles. The stress intensity is calculated using 9 from the principal stresses.

$$[\sigma_{ij}] = \max\left(\left|\sigma_1 - \sigma_2\right|, \left|\sigma_2 - \sigma_3\right|, \left|\sigma_1 - \sigma_3\right| \right) \tag{9}$$

The maximum interim alternating shear stress is then calculated using equation 10.

$$\sigma_{ij}^{d} = \frac{[\sigma_{ij}]}{2} \tag{10}$$

The maximum alternating shear stress is given by equation 11

$$\sigma_{ij} = K_e \, \sigma_{ij}^{d} \tag{11}$$

K_e assumes a value of unity in the elastic range.

3.3.6. Palmgren –Miner rule

The Palmgren –Miner rule for cumulative fatigue damage states that fatigue failure occurs when the number of applied load cycles exceeds the pertinent fatigue life expressed in terms of load cycles. To obtain the equation for Miner's rule, it is assumed that the amount of damage in a material at a particular load depends only on that load during an oscillation.

Moreover, each specimen of the same material undergoes the same extent of damage and, lastly, the total damage that a specimen accrues, due to a sequence of load cycles, is equal to the sum of damage accrued at each specific load oscillation. On the basis of the aforementioned assumptions, an equation for defining the cumulative damage due to fatigue was developed using equations (12) and (13)

$$W = N_i w_i \tag{12}$$

$$\sum_{i=1}^{k} n_i w_i = W \tag{13}$$

$$\sum_{i=1}^{k} \frac{n_i}{N_i} = 1 \tag{14}$$

where W is the total damage at failure, w_i is the amount of damage for one repetition of the load, n_i is the number of applied load cycles and N_i is the number of load cycles to failure. For each specific load step, depending upon the number of loading cycles, a damage factor is obtained. The summation of all the damage factors obtained for each of the load cases, gives the cumulative damage factor that accounts for the total damage that the artery undergoes. The Palmgren-Miner rule is an efficient tool which provides an estimation of the maximum number of cycles of loading that an object might be subjected to before the initiation of fatigue damage.

3.3.7. Fatigue analysis in this study

Graphic user interface of ANSYS is used to run the fatigue module to complete the simulations for this study. Constant amplitude loading is applied to simulate the systolic and diastolic blood pressure variations within the artery. The loading type selected in the fatigue tool was R-Ratio loading with a loading ratio (R-ratio) of 1.7. Stress life fatigue analysis is chosen for

this study since the number of load cycles is greater than 10,000 and the amount of stress developed in the artery is the critical factor in determining the fatigue life of the artery. For stress life analysis fatigue material data is stored as tabular alternating stress vs life points. The S-N curve or the alternating stress vs available life graph is defined for a specific R-ratio or loading ratio to account for the mean stress, which eliminated the requirement to select any empirical mean stress correction formulas available within the ANSYS fatigue module. Multiaxial stress correction is also implemented since the experimental test data (S-N data) is uniaxial whereas stresses are usually multi-axial. This is done by setting the 'stress component' in the Options section in the fatigue tool detail view. The stress components selected for this analysis was maximum shear stress since that is one of the critical factors in determining the fatigue life of the artery. Maximum shear stress is used to compare against fatigue material data. The fatigue tool then evaluates the FE stress results using internal solver. For constant amplitude loading only one set of FE stress results along with the loading ratio is required to calculate alternating and mean stress values using equation (12) through (14). The alternating stress value is compared to the experimental fatigue data to predict the fatigue life of the artery.

3.4. Periodic boundary conditions

Periodic Boundary conditions (PBC) are a set of boundary conditions used to simulate a large system by modeling only a small part of it. PBC is applied when the properties of a system need to be studied in bulk. To apply, a small unit cell is created which, if repeated infinitely throughout space, creates the system under consideration. If one side of the unit cell is deformed, the opposite face in deformed in the same manner and to the same extent. This wave of deformation is carried on to similar faces on all the unit cells in the system. Hence, all the unit

cells behave as small molecules within a bulk. The RVE of the artery, created in this study, represented a single unit cell within a system. The unit cell of the artery was repeated infinitely along the length to produce the entire artery under consideration. The need to consider periodicity in this study is because only a very small segment of the artery of length 20 mm is considered for completing the simulations on the fatigue analysis. To ensure that the results obtained in this finite element study is a true representation of the effect of pulsatile blood pressure on the entire length of the artery; periodic boundary condition was implemented along the length of the artery. In this study, periodicity was, therefore, only considered along the length of the artery. To implement periodicity along the length of the unit cell the circular cross sections of the model were periodically constrained in all three of the co-ordinate directions. All the nodes on one of the circular cross-section faces of the model were constrained with coincident nodes on the opposite face by implementing a set of constraint equations. The constraint equations were so formulated, so as to ensure identical deformation on both the faces. This was achieved by constraining the degree of freedom (df) of coincident nodes on the two surfaces. In the constraint equations used to implement PBC, U_i (i=x, y, z) represented displacement in the co-ordinate direction and N_1 and N_2 represented node pairs on opposite faces [30].

$$U_x^{N2} - U_x^{N1} = 0 \tag{15}$$

$$U_y^{N2} - U_y^{N1} = 0 \tag{16}$$

$$U_z^{N2} + U_z^{N1} = 0 \tag{17}$$

Application of PBC alone will cause rigid body motion in the model. To avoid rigid body motion, additional constraints were applied on the unit cell. The nodes on the circular cross-section of the artery, at the center of the arterial length, were constrained. The nodes parallel to the Y-axis were constrained in the X and Z directions while the nodes parallel to the X-axis were

constrained in the Y and Z directions. All the other nodes in the artery remained free to deform. The applied constraints ensured that stress concentration, or localized stress development, did not occur in the model, but, at the same time, rigid body motion was prevented. These constraints helped to simulate a real world environment.

3.5. Loading

Load applied on the artery was intraluminal blood pressure. This was applied in the form of pressure on the inner surface of the artery. The blood pressure was pulsatile in nature and, hence, to simulate the actual physiological loading conditions within the artery, a cyclic load in the form of systolic and diastolic blood pressure was applied. There were two different sets of blood pressure used in this study [47]: 1) normal blood pressure and 2) hypertensive blood pressure. Table 3 gives the blood pressure levels that were considered for the simulation

Table 3. Transient loading values: normal and hypertensive blood pressure

Time(sec)	Normal blood pressure(KPa)	Hypertensive blood pressure(KPa)
0.0001	9.47	12.8
0.2001	17.1	22
0.8001	9.47	12.8

The blood pressures used for this simulation were obtained from radial arteries. Radial arteries have almost the same diameter and a thick muscular wall like in coronary arteries [47]. Radial arteries have also been successfully used in coronary artery bypass grafting. Since radial arteries are anatomically similar to coronary arteries, the pulse pressure variation within these arteries was used effectively in this study.

3.6. Material properties

The coronary artery was modeled as a non linear elastic material in this study [48]. Uniaxial tests done on porcine coronary artery samples revealed a non linear stress strain graph. An initial linear elastic region, where elastin was the primary load bearing structure, was followed by a toe region. In this region, the undulated collagen fibers straightened and, hence, a large deformation was observed at low stress. In the final linear region, the collagen fibers acted as the load bearing structure. The elastic properties of the artery [48], along with the experimental uniaxial non linear data, were used to define the artery as a non linear elastic material. The non linear elastic material properties of the artery are summarized in Table 4 and Figure 8.

Table 4. Elastic properties of normal and hypertensive arteries [47]

Properties	**Normal artery**	**Hypertensive artery**
Young's Modulus (MPa)	2.68	2.25
Poisson's Ratio	0.49979	0.49979
Bulk Modulus (MPa)	490.35	490.35
Density (kg/m^3)	1.13	1.13

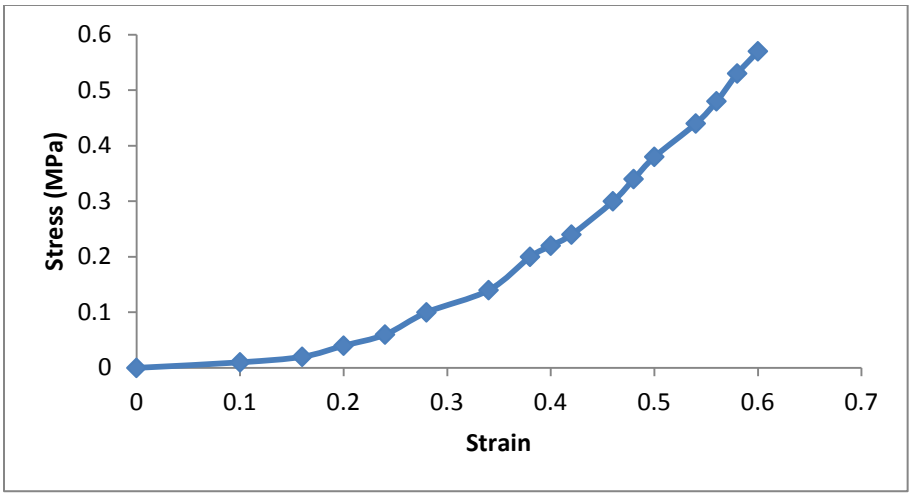

Figure 7. Non linear uni-axial experimental stress vs strain data for artery [48]

For fatigue analysis of arteries the S-N graph was defined for a specific R-ratio. For this analysis the experimental data was obtained by subjecting samples of porcine tissue to various levels of cyclic stress ranging from normal human blood pressure of around 13KPa to 5MPa [49]. The effects of loading, which is expressed by the R-ratio = P_{MAX}/P_{MIN} played a crucial role in determining the fatigue response of arteries in this analysis. An R-ratio of 1.7 was chosen for this purpose which was the ratio of the systolic to diastolic blood pressure. The mean stress for the S-N curve at 1.7 R- ratio was calculated and accounted for internally by the ANSYS fatigue solver module. The alternating stress versus life cycle data is summarized in Figure 9.

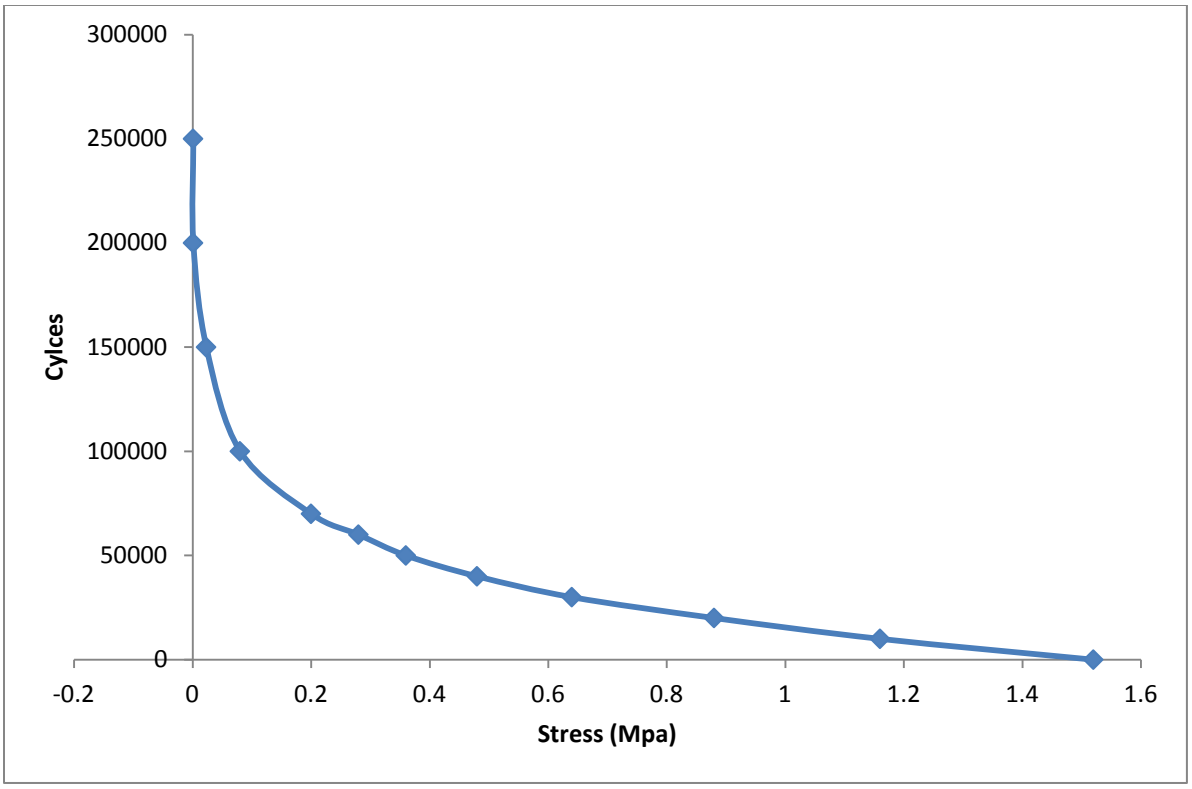

Figure 8. S-N graph data for artery [49]

Another important aspect of the study involved the comparison of the fatigue properties of arteries for different age groups. The FE simulations, completed for this comparison, encompassed the morphological and biomechanical changes occurring in the artery with age. Van der Heijden-Spek *et.al* [37] obtained the stiffness of the male coronary artery was observed to vary for different age groups starting from a day old infant to a 59 year adult. The Young's modulus of the artery, for different age groups, utilized in this parametric study is summarized in Table 5.

Table 5. Elastic modulus of artery for different age groups [37]

Age Group	Age (Years)	Young's Modulus (MPa)
1	0-1	1.17
2	1-7	1.12
3	8-19	0.9
4	20-39	1.57
5	40-59	2.19

The surrounding tissue was modeled as a linear elastic material [50] with properties summarized in Table 6. The yield stress [51] for tissue material was assumed to be the constant value of alternating stress for simplicity in simulation results. This assumption was made since no direct load was applied on the tissue material; it is effect of the stiffness of the tissue material on the amount of stress and consequently the fatigue life of artery that is the focus of this study.

Table 6. Elastic material properties of surrounding tissue material used in the finite element model [50]

Properties	Values
Elastic Modulus (KPa)	66.7
Poisson's ratio	0.48
Density (kg/m^3)	1.04
Yield Stress (KPa)	20

CHAPTER 4. FATIGUE RESPONSE OF ARTERIES

Four different aspects of fatigue response were analyzed in this study. The first part of the parametric study is aimed at analyzing the fatigue response of arteries under hypertension with a variation in mechanical properties. Hypertension is the condition when the pressure of the blood flowing through the artery increases beyond the normal range. Progressive weakening of the arteries with age causes greater stress to develop on the arterial wall. Development of plaques on the inner arterial wall resulting in constriction of the artery diameter also contributes to increased blood pressure within the artery. Hypertension is accompanied by arterial dilation along with an increase in wall stiffness. For this study it was assumed that the internal diameters and thickness of both normotensive and hypertensive arteries were similar.

In the second part of the parametric study involving the study of the effect of age on the fatigue response of male coronary arteries, arterial remodeling in the form of variation in arterial stiffness, external diameters and thickness of artery were all taken into account. Shear stress development and its effect on the fatigue life of an artery were analyzed in the study.
Arterial undulation is a phenomenon which has been observed to occur under various abnormal conditions. Pressure variations within the artery in the form of hypertension; or loss of pressure and morphological changes in the artery due to ageing, or disease, leading to reduced arterial stiffness and weakened arterial wall, may lead to arterial undulation. The effect of the deformation or bucking in the arterial structure on its mechanical response has not yet been previously analyzed. This study aimed at analyzing the stress concentration patterns due to undulations developed in the artery and the subsequent effect on fatigue life by developing an FE model for an undulated artery.

The artery functions under different types of physiological pressures in vivo like that of surrounding tissue material, or organs. It becomes crucial, therefore, to understand the effect of this factor on the fatigue response of the artery. Tissue material mimicking gelatin was used to understand the effect of the surrounding stiffness on the mechanical properties like Young's modulus of the artery. In this FE study, the surrounding tissue material was modeled as an elastic material for computational simplicity and its effect of the fatigue response of the artery was observed.

The results are expressed in form shear stress plot and fatigue life. Maximum shear stress developed in the artery is a critical factor in determining the life of the artery. The constant physiological cyclic loading of the blood pressure within the artery results in the development of shear and normal stress within the walls of the artery. The pressure on the inner face of the artery is higher than that on the outer face which brings into effect a shear force between the walls of the artery. Normal stress developed in the artery in the perpendicular directions is low since the the blood pressure is under physiological limits and over a the life time of the artery it's the effect of the shear stress that results in the development of fatigue damage within the artery.

4.1. Assumptions in the finite element study

- The artery originally is made up of three different layers composed of different amounts of elastin, collagen fibers and smooth muscle cells. This study simulated the artery as a single layered structure neglecting the contributions of the individual layers in arterial remodeling.

- The artery was simulated as a non linear elastic material for the FE simulation completed in this study. No definite conclusion has been made in the literature regarding the material type used for arteries.
- The surrounding tissue material was modeled as a linear elastic material. This was done for computational simplicity, since very little stress develops in the tissue material due to physiological intraluminal blood pressure loading within the artery. Moreover the fatigue response and stress development within the artery was the primary focus of this study and the material formulation of surrounding tissue material was, therefore, kept simple.
- The SN graph used in this study was obtained after cycling porcine coronary artery samples to failure [49]. The tissue material was cycled upto two million cycles for a stress level of 0.4 MPa. The final S-N graph is an exponential approximation of the results and may not be a true representation of the in vivo response of arteries.
- The S-N graph for connective tissue material was not available in the literature and the yield stress for tissue material was considered, therefore, to be the constant alternating stress over the entire range of life cycles for the purpose of the simulations.

4.2. Effect of hypertensive arteries subjected to high blood pressure on shear stress accumulation and fatigue life of arteries

The literature review of the properties of hypertensive arteries suggested increased arterial stiffness of the artery with increase in blood pressure levels due to smooth muscle cells, simulated collagen fiber accumulation, and fatigue failure of load bearing elastin fibers [31-35].

4.2.1. Finite element simulation results:

FE simulations were completed to analyze the difference in fatigue response of hypertensive and normotensive arteries in this study. Two aspects of hypertension were considered:

1. Increase in blood pressure within the arteries and;

2. Variation in stiffness of the arterial wall

The results of the study indicated increased shear stress concentration in the arteries due to hypertension. Total deformation in the normotensive artery was observed to be 3.58% lower than the hypertensive artery. Maximum deformation was observed on the outer edges of the artery as shown in the figures 10 and 11.Increased intraluminal blood pressure contributed to the increase in deformation in the hypertensive artery. The maximum shear stress in normotensive arteries was observed to be 26% lower than that in hypertensive arteries. The stress accumulation pattern was observed to be the same for both the arteries with maximum shear stress concentration on the inner wall of the artery and minimum stress on the outer wall as indicated in figures 12 and 13. Stress was observed to reduce circumferentially but remain constant along the length of the artery. The extent of increase in total deformation is small compared to the extent of increase in shear stress which indicates that the stiffness of the hypertensive artery is higher compared to normotensive artery at increased pressure. It is also observed that the extent of shear stress concentration is inversely proportional to available fatigue life, with the increase in the stress concentration the fatigue life is observed to decrease. The maximum available life for normotensive arteries was higher by 1.85% when compared to hypertensive arteries. The results indicated that increased blood pressure and stiffness of hypertensive arteries lead to the development of increased shear stress and decreased available fatigue life.

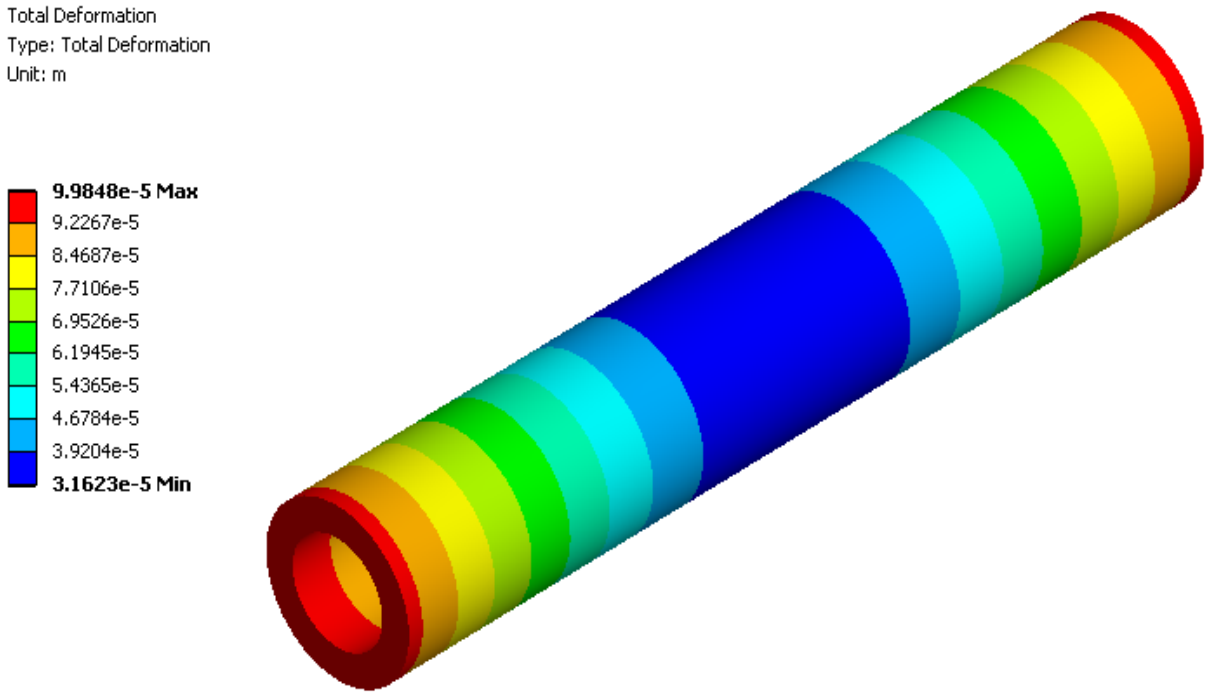

Figure 9. Total deformation in normotensive arteries at normal blood pressure transient loading

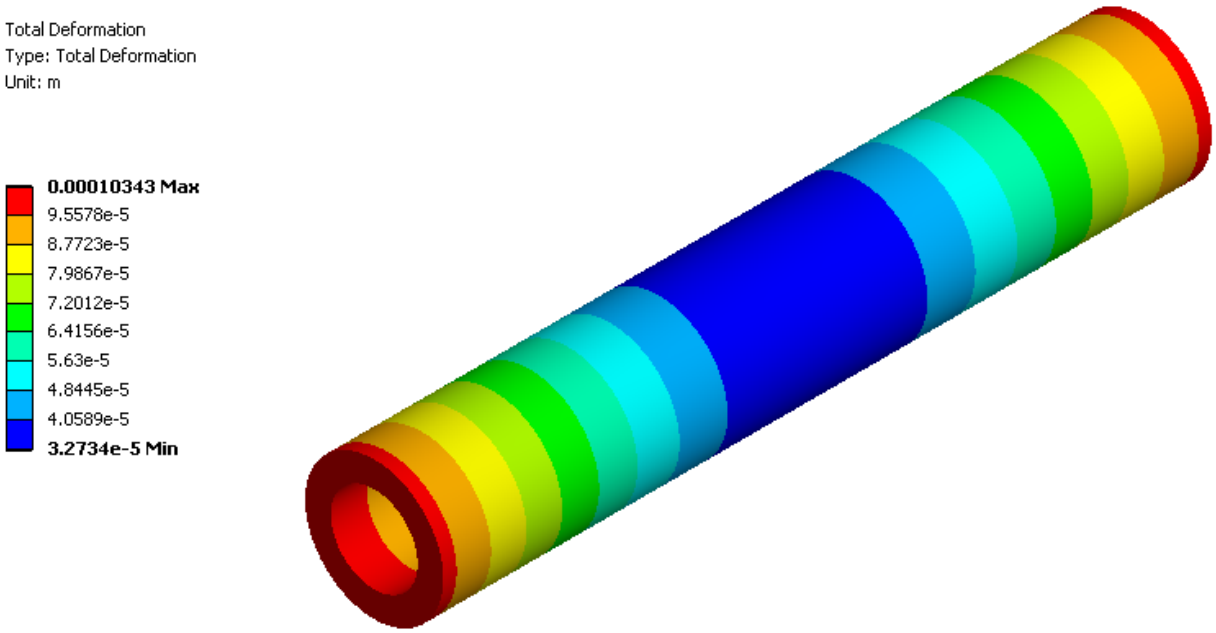

Figure 10. Total deformation in hypertensive arteries at high blood pressure transient loading

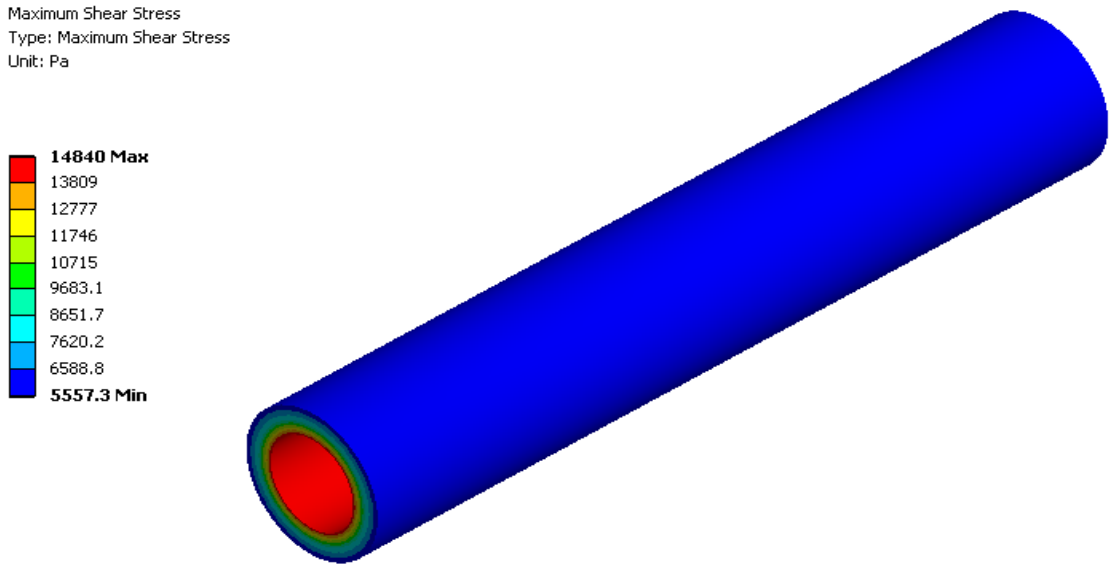

Figure 11. Maximum shear stress accumulation in normotensive arteries with normal blood pressure transient loading

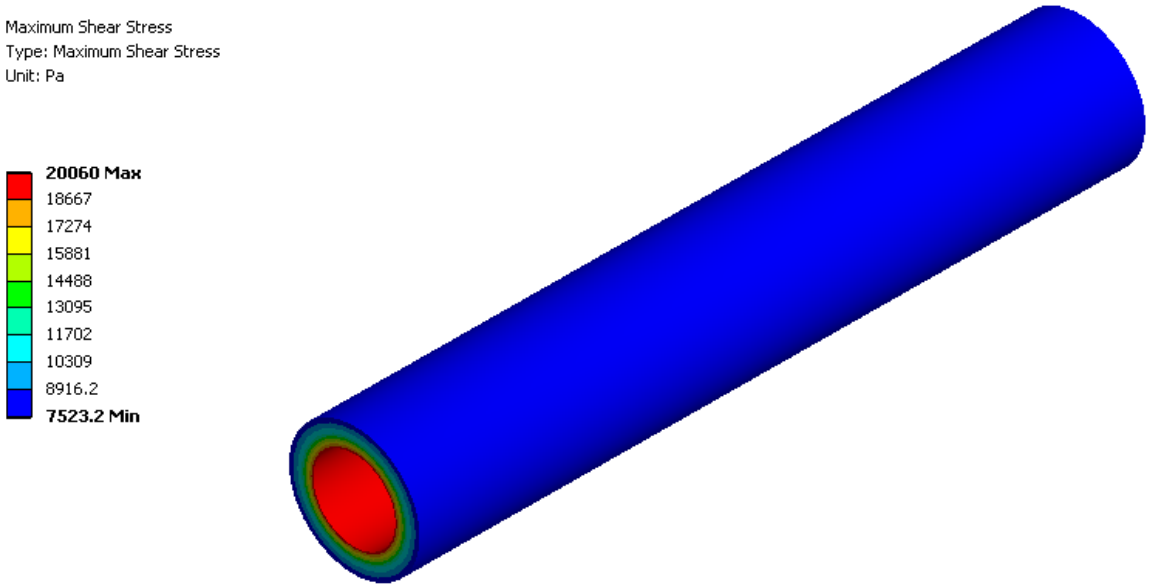

Figure 12. Maximum shear stress accumulation in hypertensive arteries under high blood pressure transient loading

4.2.2. Verification of results

The FE results obtained for human coronary artery in this study indicated shear stress accumulation in normotensive artery to be 26% lower than hypertensive artery. Higher intraluminal blood pressure and increased stiffness of artery contributes to the increased stress accumulation in hypertensive arteries. Pourageaud *et.al* [56] compared the stress strain response and variation of the incremental elastic modulus of conductance coronary and mesenteric arteries from spontaneously hypertensive rats (SHR) and Wistar Kyoto rats (WKR) with normal vessels using an arteriograph system. Their results indicated shear stress in normal WKR artery to be 37% lower than SHR artery. The finite element study indicated lower variation in shear stress between hypertensive and normal arteries compared to experimental due to different material properties, diameter and thickness of the arteries .

Stress life analysis in the ANSYS Fatigue module for a constant amplitude load application used in this study calculates the alternating stress developed in the system at a certain load and interpolates the result to calculate the life available in terms of number of available load cycles at that stress level from the S-N curve [25]. Hence the FE results can be considered to be an approximate estimate of the variation in fatigue life of artery due to hypertension.

4.3. Effect of ageing on shear stress accumulation and fatigue life of arteries

Mechanical properties of arteries have been observed to change with age. Various investigations have revealed alterations in biomechanical properties of the arteries and structural remodeling that lead to variation in mechanical response of arteries with age. Both of these aspects were considered in this FE study to analyze the effect of these morphological changes on the fatigue response of arteries over their life span.

4.3.1. Finite element simulation results

The effect of change in elastic modulus and arterial wall thickening was analyzed by studying its effect on the extent of total deformation, shear stress and fatigue life of arteries. For age groups 1 through 3, decrease in elastic modulus contributed due to the decrease in the content of collagen fiber in the artery and, thereby, a possible increase in distensibility of the artery. Reduced elastic modulus would, consequently, lead to reduced arterial stiffness [36]. The effect of a decrease in arterial stiffness is reflected in the results of the FE simulation. The shear stress developed in the arteries was observed to decrease for age groups 1 and 2. For the third age group, the shear stress increased though the elastic modulus decreased. This can be attributed to the increased internal surface area of the lumen at this stage and reduced rate of arterial thickening from age group 2 to 3. The thickness of the arterial wall increased from 0.2mm to 0.4 mm from age group 1 to 2, but then increased very slightly to 0.43mm in age group 3. The arterial diameter kept increasing with age, but the rate of compensation, in the form of arterial wall thickening, was slow which could be attributed the increase in stress levels for age group 3 inspite of reduced stiffness levels. Beyond group 3, the elastic modulus for the artery increase, but for age group 4, the shear stress level decreased and then increased again with further progression of ageing of the artery. Astrand *et.al* [57] performed an in-vivo study to analyze the age related increase in wall stress of the human abdominal aorta. He concluded that arterial diameters increase with age which is compensated by arterial wall thickening simulated by the smooth muscle cells that trigger the production of collagenous matter.

It can be intepretated, therefore, that since the extent of arterial thickening and increase in collagenous content in the arterial wall does not effectively compensate for the increase in arterial diameter, there is a reduction in shear stress level. The results obtained from the

simulation in this study indicate a fluctuation in shear stress levels over the different age groups. The maximum shear stress level is observed, however, to develop in the artery for age group 1 where the thickness of the arterial wall, and the stiffness, is the least due to less collagen content in the artery. The extent of deformation is inversely proportional to the elastic modulus of the artery except for the age group 2 where a sudden decrease in deformation is noticed though the elastic modulus decreases. Increased rate of arterial thickening might result in decreased deformation at this stage. Deformation is observed to be minimum near the central region of the arterial length and maximum at the edges. Fatigue life of the artery was observed to be inversely proportional to the shear stress developed in the arterial wall, and an increase in the shear stress accumulation results in a decrease in the fatigue life of the artery. Maximum life is available on the outer surface of the artery, while minimum life is available on the inner surface where the intraluminal blood pressure is applied. Figure 19 shows that arterial fatigue life is the least for age group 3. Fatigue life of an artery is observed to vary only in the circumferential direction and it remains constant along the length of the artery. The extent of arterial remodeling, or the rate at which collagenous tissue and extracellular matter is produced, is age dependant indicated by the variation in thickness of the artery and the elastic modulus with age observed by Ozonlanta *et.al* [36] in their experimental results . This would result in fluctuations in the extent of shear stress development over the different age groups and directly affect the fatigue life of the artery.

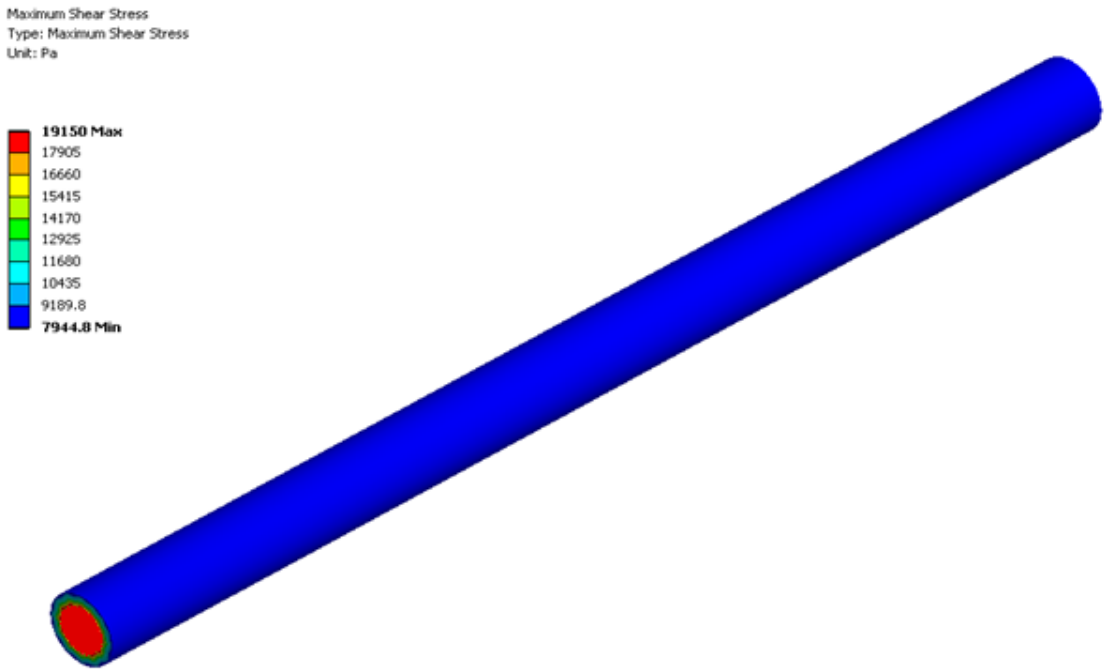

Figure 13. Maximum shear stress distribution for age group 1

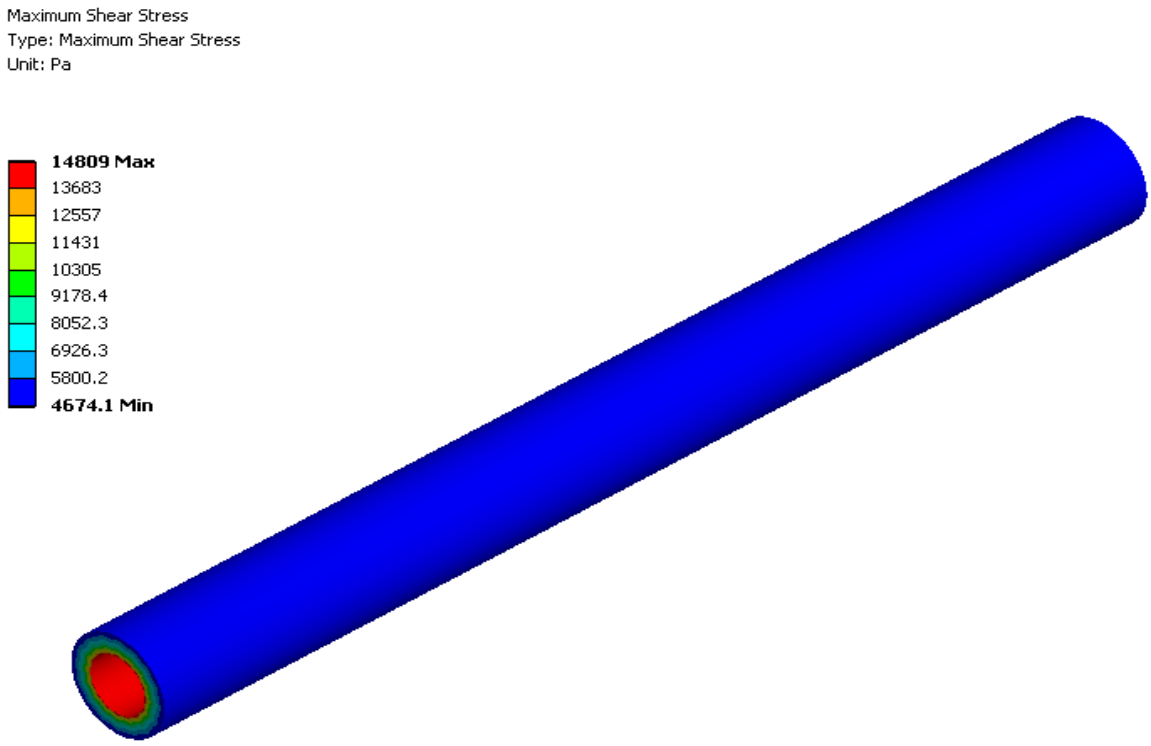

Figure 14. Maximum shear stress distribution for age group 2

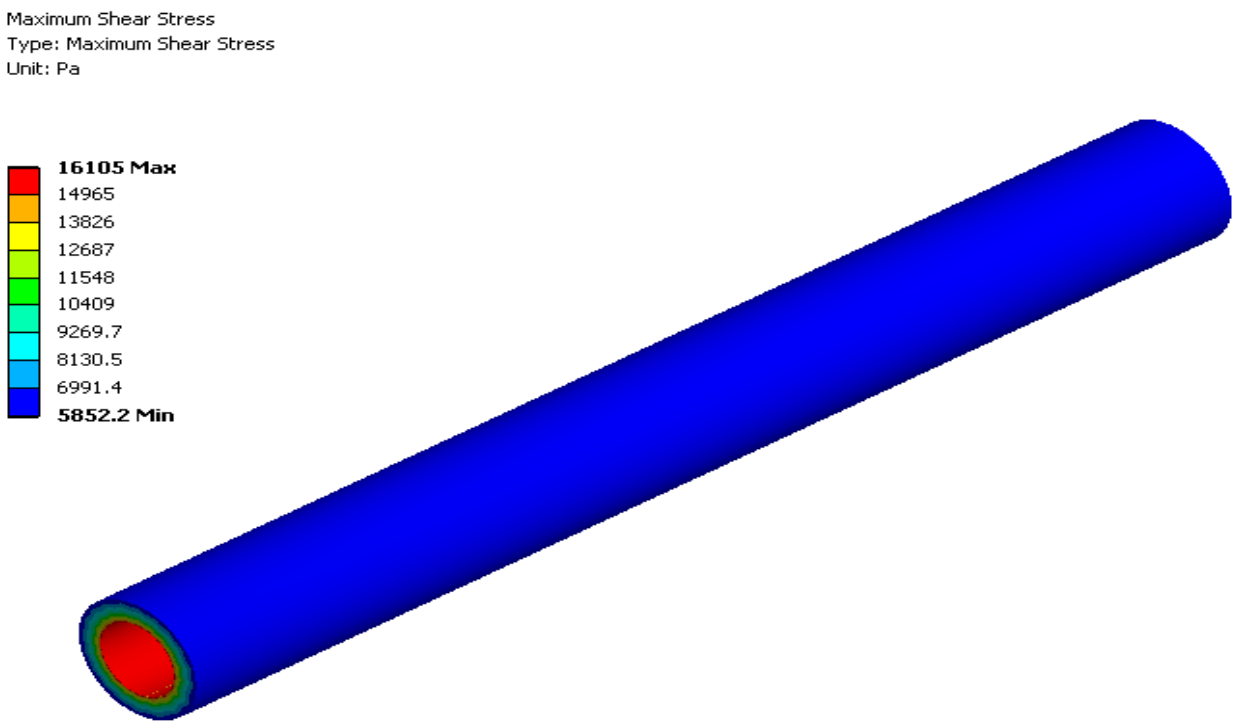

Figure 15. Maximum shear stress distribution for age group 3

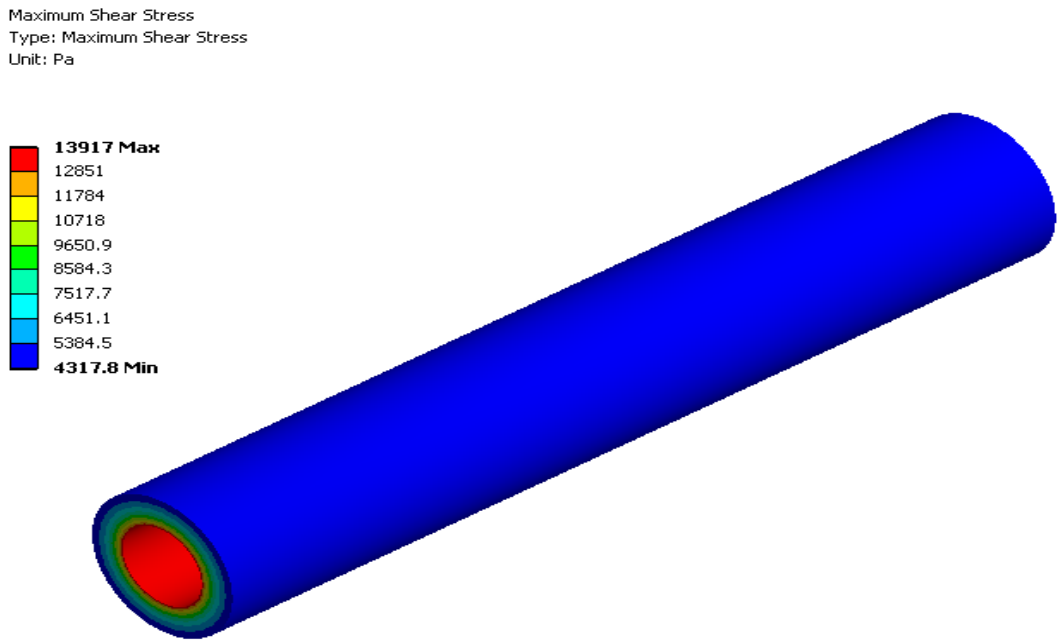

Figure 16. Maximum shear stress distribution for age group 4

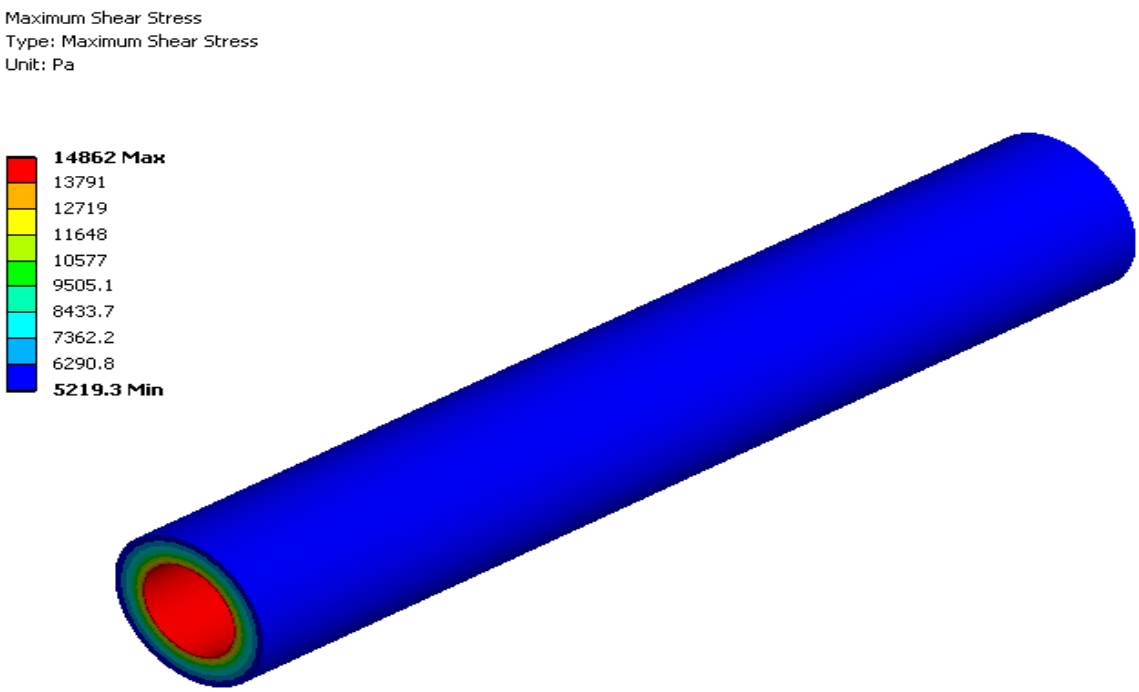

Figure 17. Maximum shear stress distribution for age group 5

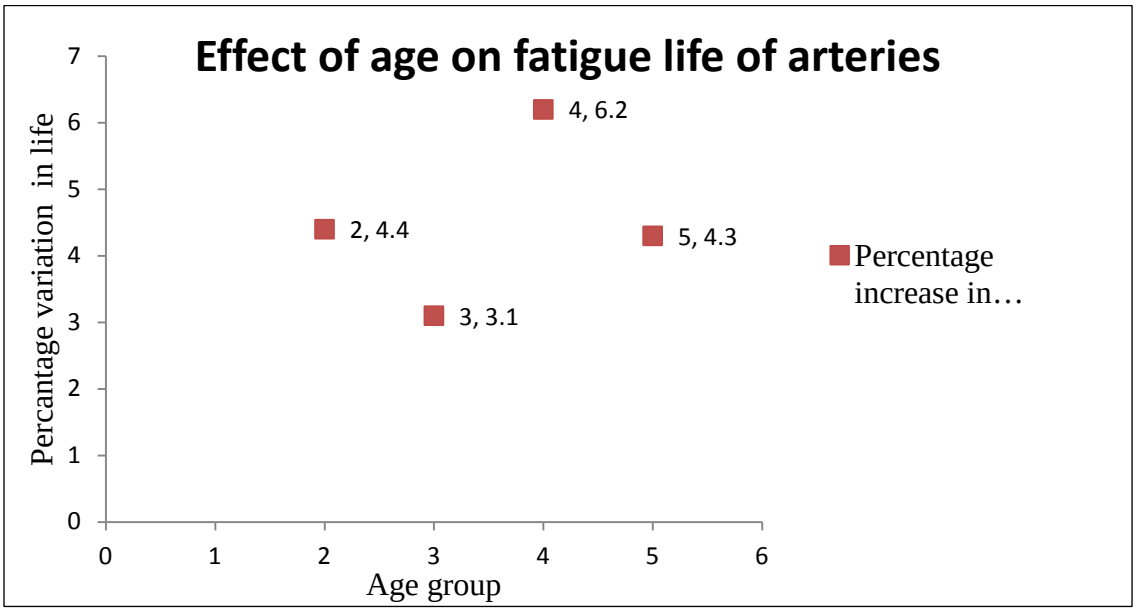

Figure 18. Percentage variation in minimum life of arteries for age groups 2 to 5

4.3.2. Verification of results

The FE analysis results indicated a decreasing trend in the maximum shear stress accumulation within the artery with increase in age through age 1 to 5. The decreasing trend is found to be in comparable to experimental results obtained by Samijo *et.al* [58], where the variation in wall shear stress in common carotid artery was investigated as a function of age. Wall shear stress is the stress developed on the innermost surface of the vessel due to the drag exerted by the flowing blood. Samijo et.al used an ultrasonic system to measure the wall shear rate which was used to assess the whole blood viscosity and wall shear stress using numerical approximation proposed by Weaver *et.al* [59]. The results obtained in their study indicate an 18% decrease in wall shear stress. The FE results obtained in this study is a measure of the shear stress developed on the circumferential plane of the artery due to the intraluminal transient blood pressure. The FE results indicated a 22.4% decrease in the maximum shear stress from age group 1 to 5. Though a decreasing trend in the maximum shear stress accumulation was observed in the finite element results, one of the important interpretations of the results is that both the extent of arterial wall thickening, arterial dilation and stiffening with age has a combined effect of the extent of shear stress accumulation in the artery. The fatigue life of artery was observed to increase with age as a consequence of decrease in stress accumulation within the artery. The observations made in the finite element results suggest that arterial remodeling in form of increased arterial diameter and thickness compensates for the increased arterial stiffening with age and hence results in decrease in stress accumulation in arteries.

4.4. Effect of arterial undulation in the form of undulation amplitude on shear stress accumulation and fatigue life of arteries

Arteries have been observed to kink, or buckle, under various physiological conditions like hypertension, reduced axial strain and a weakened arterial wall. Arteries have also been observed to buckle under the effects of age. Han [60] developed a biomechanical model to represent arterial undulation. He concluded, from his experimental results, that critical pressure leading to the undulation of arteries was dependant on elastic modulus of the wall, diameter, length and thickness of the artery, and that axial strain developed in the arterial wall. This FE study aimed at analyzing the variation in fatigue response of arteries due to different extents of undulation.

4.4.1. Extent of undulation

The extent of undulation in the artery is expressed in terms of undulation size and undulation amplitude. The undulation size is the ratio of the buckled length of the artery to the original length. The undulation amplitude is amplitude of the wave created in the FE model of the artery. Four different amplitudes of undulation were analyzed in this study to better understand the effects extent of undulation on available fatigue life. The results were compared to a normal artery without any undulation.

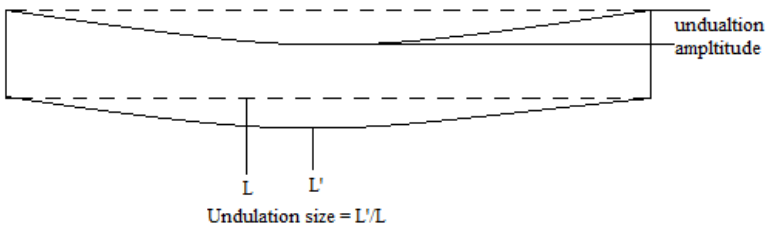

Figure 19. Representation of undulation size and amplitude of buckled artery

4.4.2. Finite element simulation results

The simulation results indicated increased stress accumulation in arteries due to undulation. Because of arterial undulation, one part of the arterial wall experienced compressive load while the opposite part was stretched and, therefore, experienced tensile load. For the artery void of any kinking, or undulation, maximum shear stress development was uniform throughout the inner wall of the artery and no stress concentrations were observed on the arterial wall along the longitudinal direction. Shear stress varied only in the circumferential direction. Change in arterial structure, in the form of undulation, resulted in stress concentrations. Unlike the normal arteries where uniform minimum stress developed on the outer circumferential surface of the artery, the stress concentration was observed to increase in the regions under compression. The rate of increase in shear stress concentration was observed to be higher in the arterial regions in a state of compression as compared to the regions under a state of tension. Maximum shear stress concentration on the inner wall of the artery did not remain uniform. Greater stress accumulation was observed along the edges of the artery. The maximum shear stress developed in the artery increased with the increase in the undulation amplitude. The maximum shear stress was observed, however, to be more and more localized at higher undulation amplitudes. The shear stress developed in the artery acted as the crucial factor in determining the fatigue life of the artery. The higher the shear stress concentration, the smaller the fatigue life of the artery.
The total deformation was also observed to increase by 41.5% with the increase in undulation amplitude from 0.4 mm to 1.6 mm. The maximum shear stress for undulation amplitude 1.6 mm is observed to be twice as much as that for 0.4 mm. It can be inferred from the results that undulation or undulation causes greater deformation and higher stress accumulation in the

arteries and hence adversely affects the life of the artery. The minimum available life is observed to decrease by 16.4% with the increase in undulation amplitude to 1.6 mm.

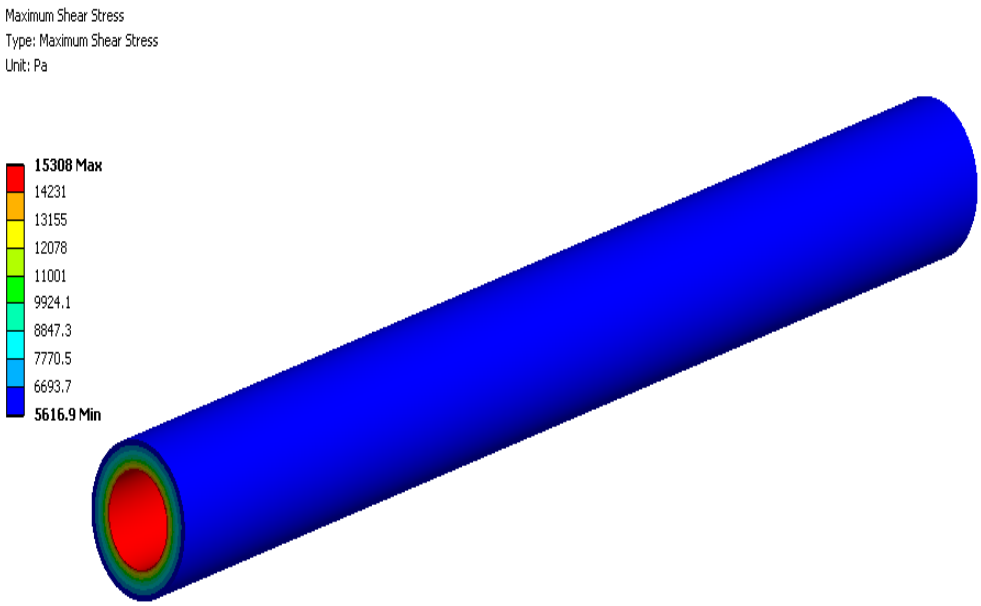

Figure 20. Maximum shear stress concentration in straight artery

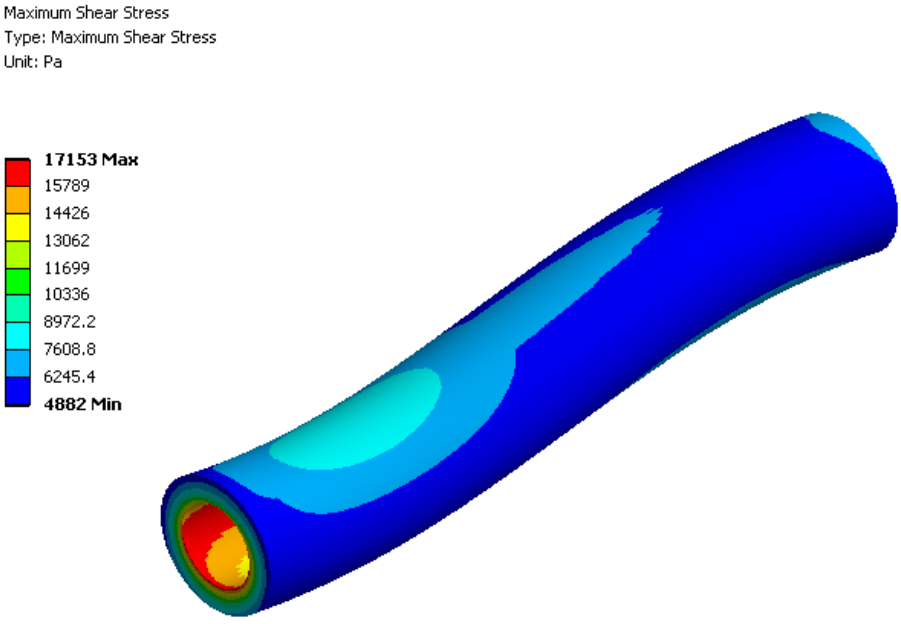

Figure 21. Maximum shear stress concentration for undulation amplitude 0.4mm

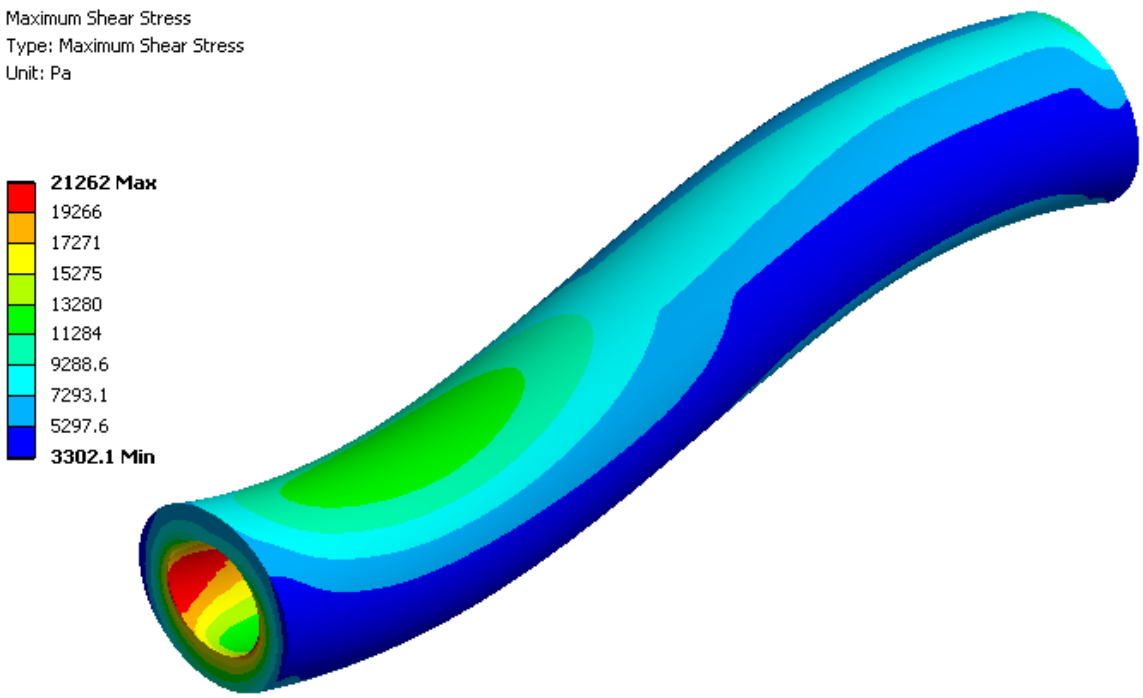

Figure 22. Maximum shear stress concentration for undulation amplitude 0.8mm

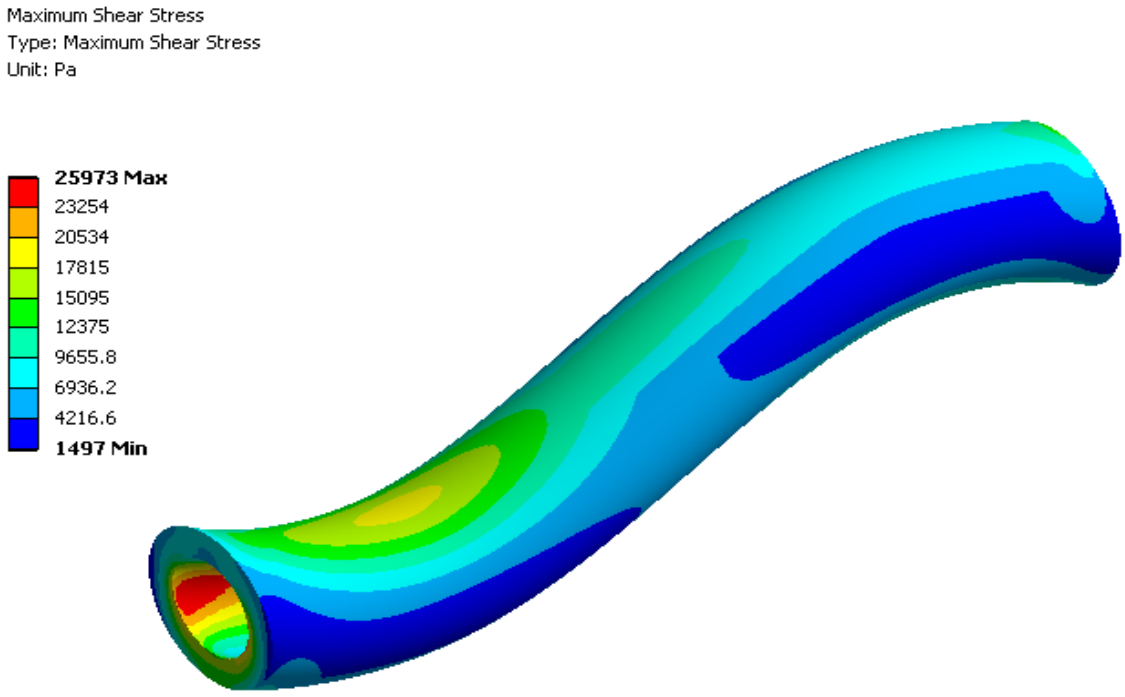

Figure 23. Maximum shear stress concentration for undulation amplitude 1.2mm

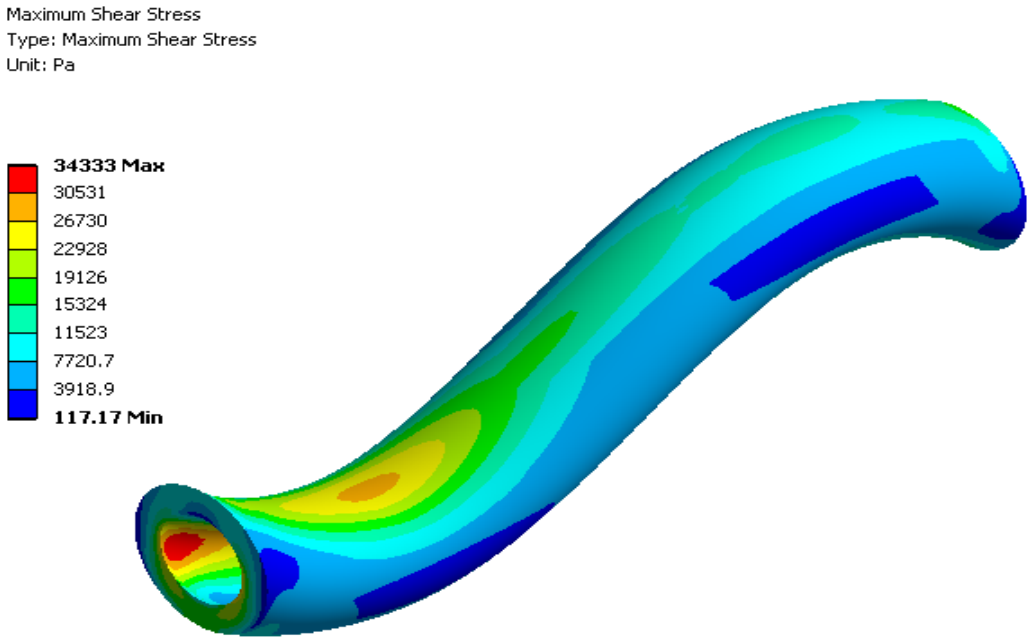

Figure 24. Maximum shear stress concentration for undulation amplitude 1.6mm

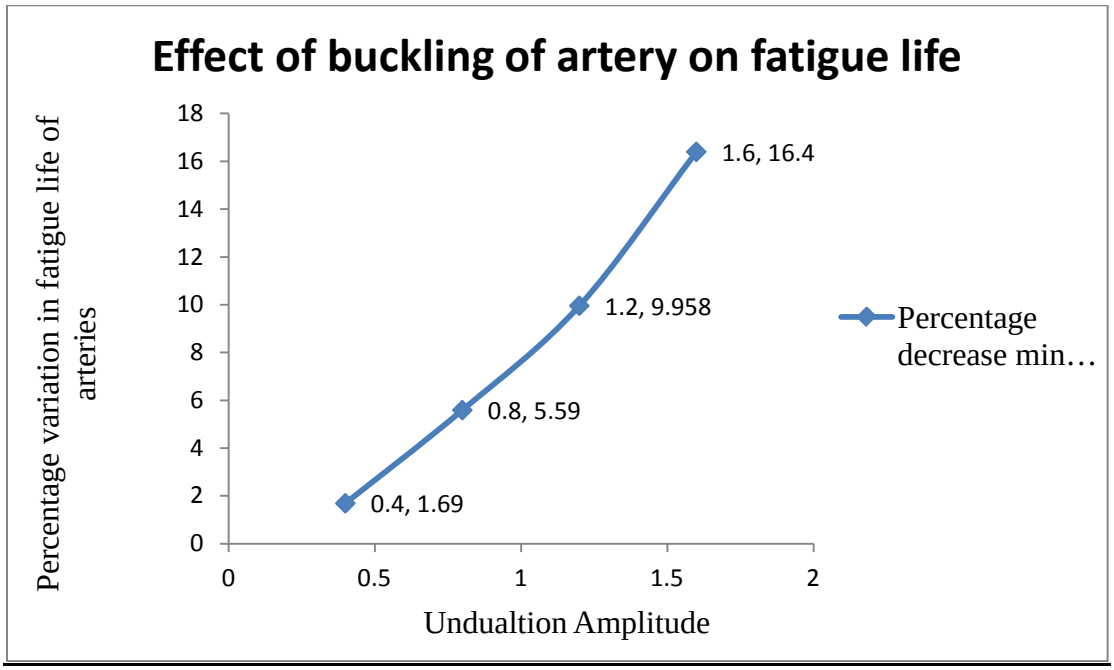

Figure 25. Percentage decrease in fatigue life of artery with increase in undulation amplitude from 0.4 mm to 1.6 mm over straight arteries

4.4.3. Verification of results

The shear stress accumulation plots in this study indicated higher stress accumulation on the inner side of the curvature compared to the outer side. This is comparable to the observations made by Johnston *et.al* [61]. Johnston *et.al* [61] in their study on analysis of effects of arterial curvature and lumen diameter on wall shear stress distribution in human coronary artery used angiographic images to reconstruct the 3D models for finite element analysis of four different coronary artery sections. To further verify the results of this study, the correlation coefficient between the undulation amplitude and the shear stress accumulation was calculated to be of the order of 0.97. This indicated a close correlation between the varying radius and curvature of the artery to the extent of shear stress accumulation. This observation is comparable to previous findings (Johnston *et.al* [61]) where the correlation index between the wall shear stress and the combined effect of varying arterial radius and curvature, was found to be 0.98. An increased shear stress accumulation was observed in the undulated arteries compared to normal arteries. The minimum available fatigue life is observed to be decrease with increase in the undulation amplitude, which is inversely proportional to the extent of shear stress accumulation within the artery.

4.5. Effect of surrounding tissue material on shear stress accumulation and fatigue life of arteries

Arteries in vivo are surrounded by loosely arranged connective tissue material. In the literature, very few studies have been conducted to illustrate the effect of surrounding tissue material on the mechanical properties of the artery. Zhang and Greenleaf [42] concluded that arteries surrounded by tissue material mimicking gelatin become stiffer. Hodis *et.al* [62]

observed an increased stiffness in the walls of the arteries modeled as viscous, viscoleastic, and stiff. In all the different arterial wall material that they observed, the maximum stress developed on the outer and inner surface of the artery and was greater for the arteries surrounded by tissue material. Han [63] developed a model to illustrate the undulation of a non linear elastic artery within linear elastic tissue material. During the development process, he also analyzed the effect of the surrounding tissue material on the extent of undulation and on critical pressure of undulation. After reviewing the simulation results and undulation equations, he determined that surrounding elastic substrate, or tissue material, increases the mode of undulation. Higher the stiffness of the surrounding tissue, the greater was the mode of undulation.

In this FE study the surrounding tissue was considered to be bonded to the artery and buckled along the axis of undulation around the artery. Moreover, the stiffness of the artery surrounded by the tissue material was considered to be the same as for the one without the tissue. In this study it has been assumed, therefore, that the elastic modulus of the artery remains the same irrespective of the surrounding tissue material.

4.5.1. Finite element simulation results

The simulation results revealed few important aspects of the effect of the surrounding tissue material on the shear stress development, as well as on the fatigue life of the arteries. The trend of the maximum stress developed within the inner wall of the artery was observed, however, to be increasing with an increase in the undulation amplitude. The minimum stress developed on the outer wall of the artery which was modeled to be directly bonded with the surrounding tissue material, and observed to follow a decreasing trendline. The variation in the maximum and minimum shear stress levels within the artery was observed to follow the same

pattern as in the artery without the surrounding tissue for different undulation amplitudes. The maximum shear stress on the inner arterial wall of the artery with the surrounding tissue material was recorded to be lower than that in the corresponding arteries without the tissue. At the same time, however, a comparison of the minimum stress levels on the outer wall of the artery, in contact with the tissue material, revealed higher levels of stress development for undulation amplitude of 0.8mm. The simulation results also indicated the maximum shear stress to be concentrated on the smaller area of the inner arterial wall for the artery without the supporting tissue material. The stress patterns on the inner wall of the artery, without the tissue, indicated greater variation in shear stress. It can be inferred from the findings that the tissue material acted as a supporting structure around the artery and reduced the extent of shear stress concentration on the inner arterial wall. At the same time, the tissue material provided a compressive load on the outer arterial wall which is the reason for an increase in the minimum shear stress level on the outer walls of the artery.

The fatigue results indicated an increase in the maximum life of the artery with an increase in the undulation amplitude. The area of maximum life concentration, however, decreased with the increase in the extent of undulation. The effect of the surrounding tissue material on the fatigue response of the artery was observed to be varied. The minimum life of the artery surrounded by tissue was observed to be decreasing until 0.4mm undulation amplitude. For higher amplitudes, however, an increase in the available minimum life of the artery was observed. The maximum available life of the artery was also observed to be increasing when surrounded by the tissue material. The varied response of the fatigue life of the artery within the tissue material could be an outcome of the various assumptions made in this analysis. The fatigue property of the tissue material, in the form of the S-N digram, was considered to be throughout

the 2.5 million life cycles of the simulation. Moreover, the variation in stiffness, due to surrounding tissue, would affect the fatigue life of the artery considerably, but was not considered in this study.

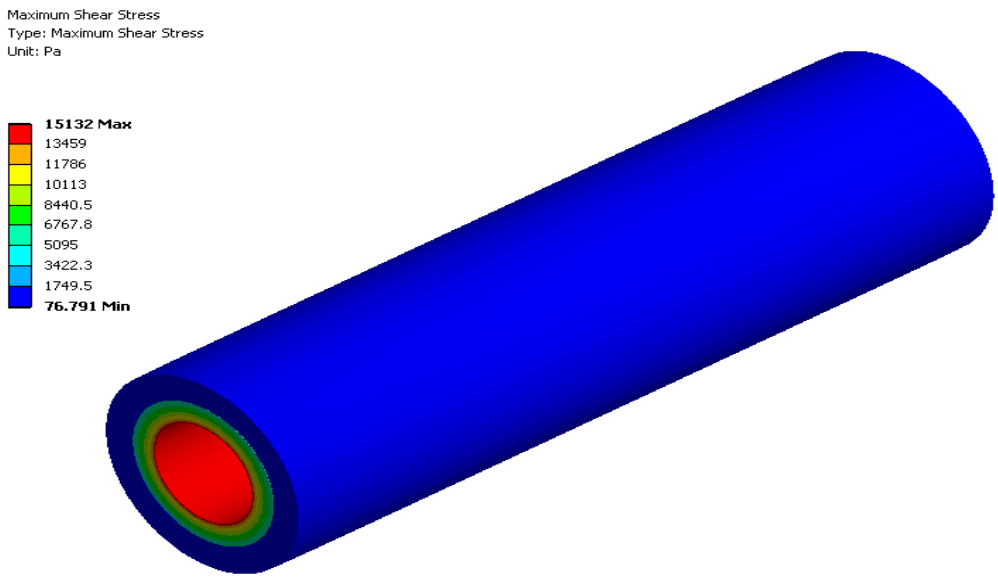

Figure 26. Maximum shear stress distribution in straight arteries with surrounding tissue

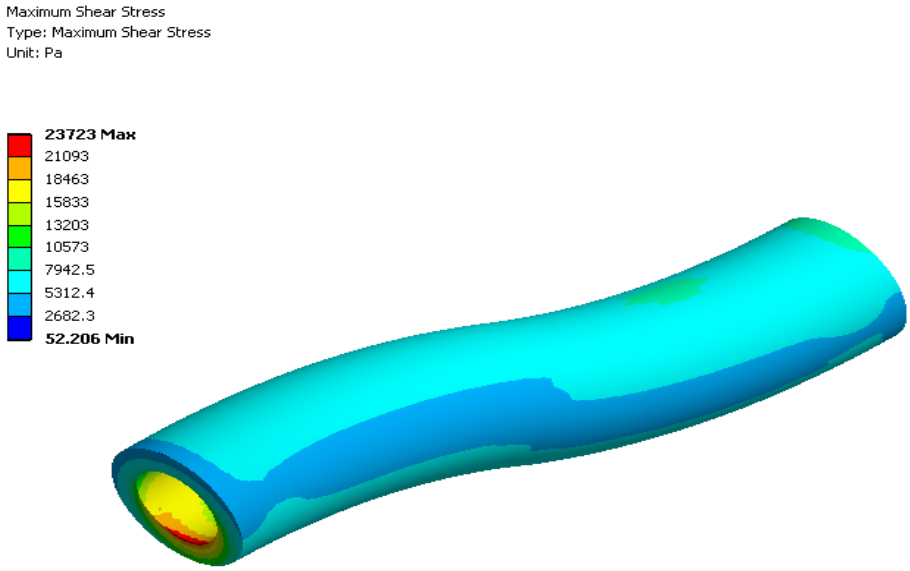

Figure 27. Maximum shear stress distribution in artery with surrounding tissue and undulation amplitude 0.4 mm

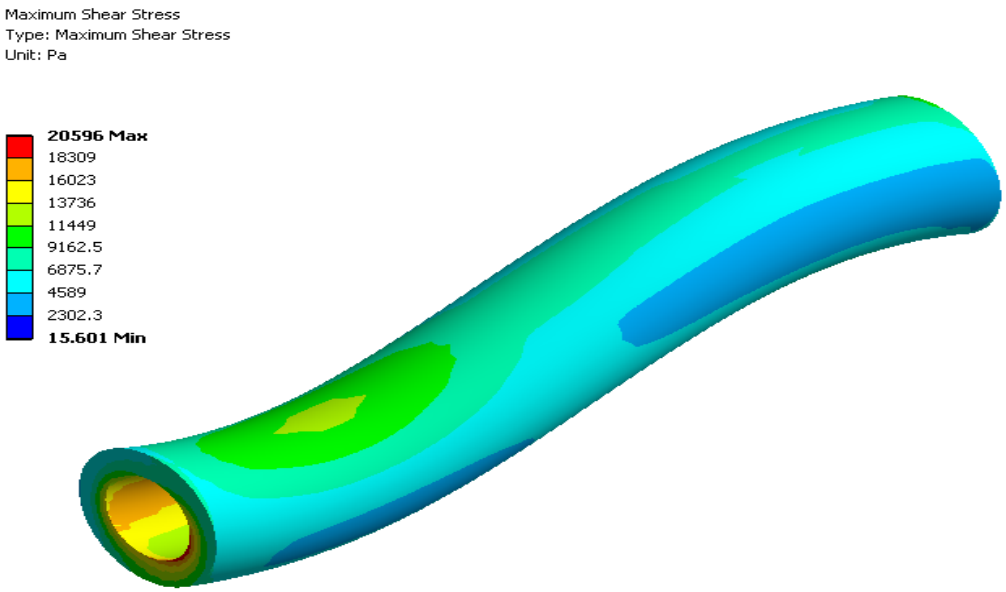

Figure 28. Maximum shear stress distribution in artery with surrounding tissue and undulation amplitude 0.8 mm

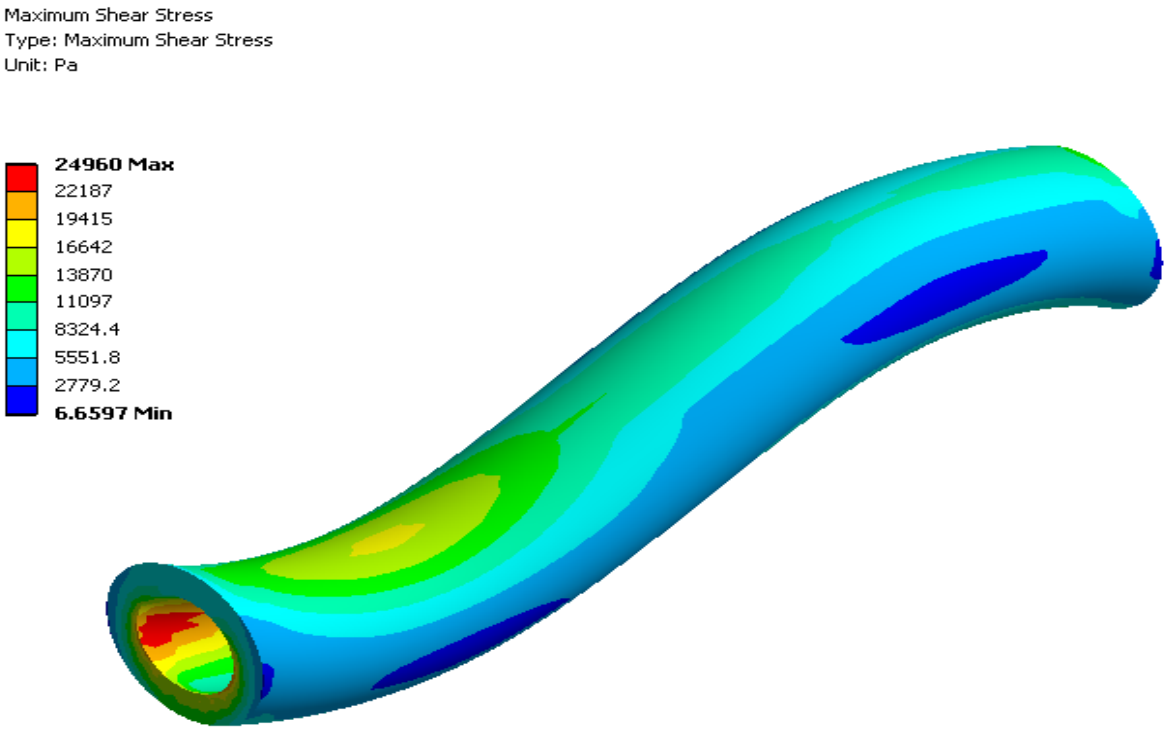

Figure 29. Maximum shear stress distribution in artery with surrounding tissue and undulation amplitude 1.2 mm

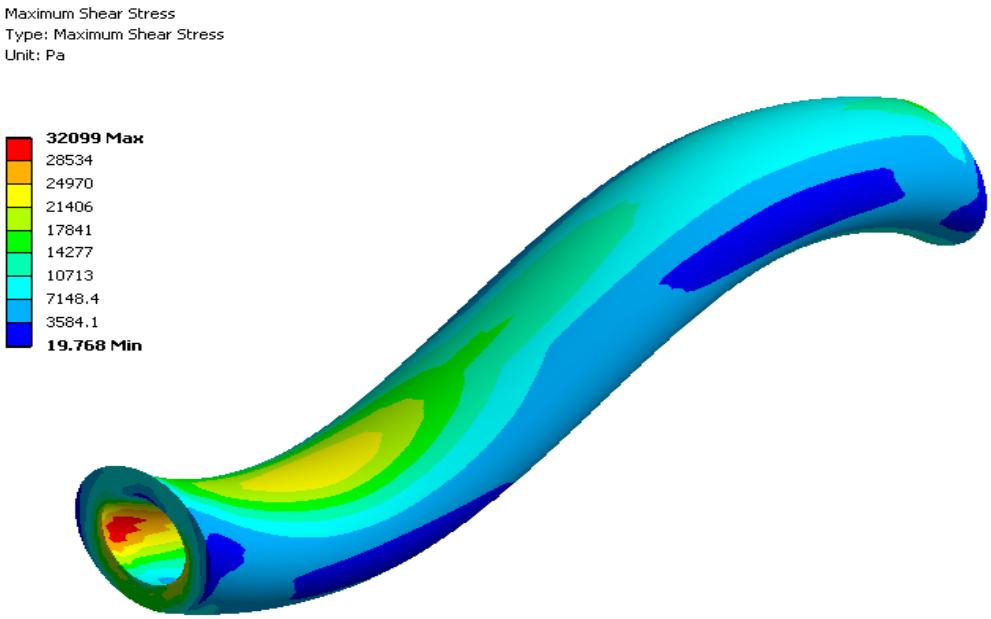

Figure 30. Maximum shear stress distribution in artery with surrounding tissue and undulation amplitude . 1.6 mm

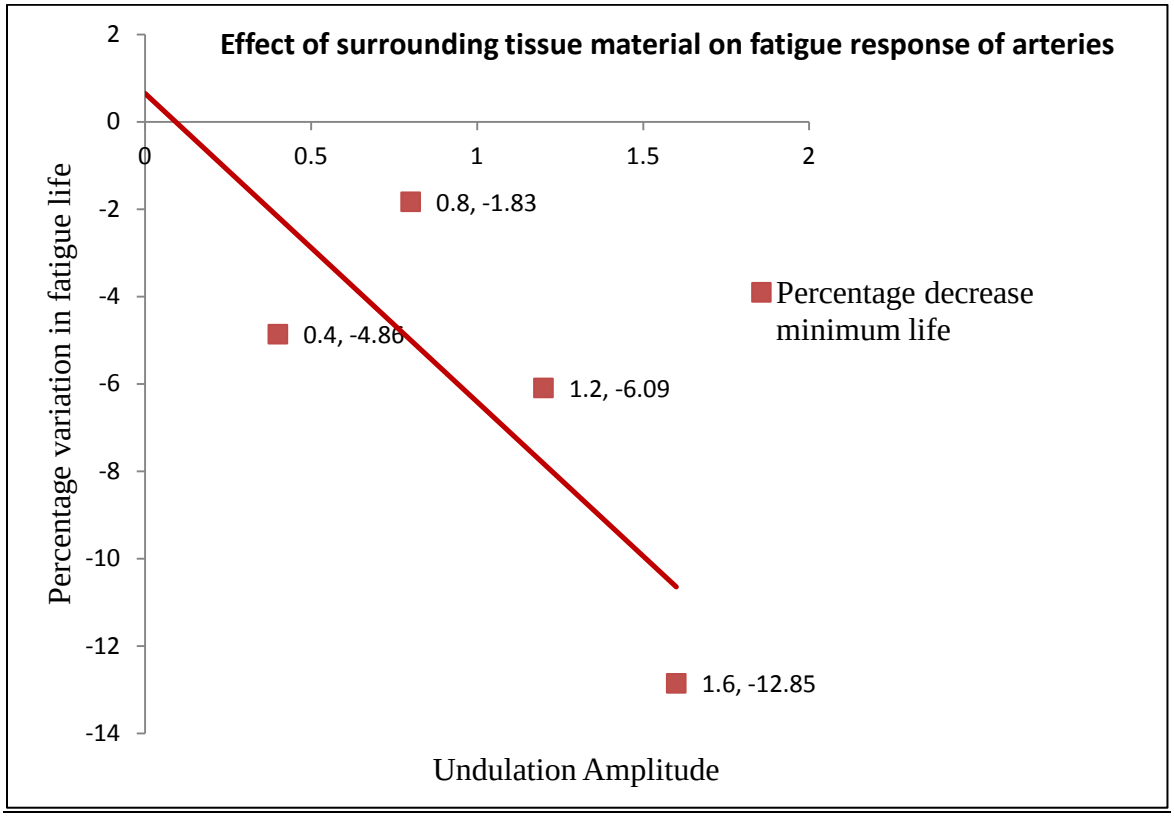

Figure 31. Percentage decrease in minimum available life of artery with surrounding tissue material for undulation amplitudes of 0.4 mm to 1.6 mm over the straight artery

3.5.2. Verification of results

A comparison of the shear stress accumulation in artery with and without surrounding tissue was completed in this study to analyze the effect of stress and fatigue response of arteries surrounded by tissue. Results revealed a higher concentration of stress in arteries without surrounding tissue for higher amplitudes of undulation. The Pearson's correlation coefficient for the shear stress results obtained in this study was of the order 0.89 which is again very close to the coefficient value of 0.87 obtained by Respetro [64] where he measured the effect of surrounding tissue mimicking gelatin on artery with shear wave dispersion ultrasound vibrometry. For straight arteries, higher stress accumulation was observed in arteries with the surrounding tissue material. Zhang *et.al* [65] observed increased stiffness in arteries with surrounding tissue material. Hence it can be suggested that stiffness of the arteries with surrounding tissue material decreases with the increase in undulation amplitude, when compared to arteries without tissue material.

CHAPTER 5. CONCLUSION AND FUTURE WORK

5.1. Conclusion

In this work FE simulations were performed to determine the stress distribution patterns and corresponding fatigue response of arteries, in the form of fatigue life, under four different physiological conditions. The finite element model created for this study was unique since periodic boundary conditions were implemented to eliminate surface effects.

The shear stress developed in the normotensive artery was observed to be 26% lower than that in hypertensive arteries. The fatigue life of the hypertensive artery was also decreased by 4.7% due to an increase in the wall shear stress levels. The available fatigue life was observed to be inversely proportional to the shear stress accumulation. Also the variation in shear stress as well as available fatigue life was circumferential.

The effect of arterial stiffening, due to age, on the fatigue response of arteries indicated the variation in the extent of arterial remodeling for different age groups. The fatigue life of the artery for different age groups was dependant on the elastic modulus, the extent of arterial dilation due to ageing, and also the rate of collagenous matter accumulation and thickening of the arteries. The minimum available life was observed to be highest for the group 4 (ages 20-39 years).

The simulation results revealed a decrease in the maximum available life of an artery with an increase in the undulation amplitude. The percentage of the decrease in minimum available life increased from 0.827 % to 30.16% for an undulation amplitude of 0.4 mm to 1.6 mm. The decrease in the fatigue life of the arteries, due to undulation, was due to higher stress accumulation in the artery caused by deformation in the arterial structure. The maximum shear

stress in the artery was observed to increase from 15308 Pa to 34333Pa for straight artery to arteries with undulation amplitude of 1.6 mm.

The effect of the surrounding brain tissue was observed to be varied for different undulation amplitudes. The minimum available life, and maximum shear stress, was observed to decrease with an increase in the undulation amplitude, as observed in arteries without the surrounding tissue material. When the minimum available life of the arteries without tissue material was compared to the response of arteries with the tissue material, an initial decrease in life, by 6.56%, was observed until the undulation amplitude of 0.4 mm. Beyond this there was a slight increase of available life.

5.2. Future work

The FE simulations completed in this study were an initial attempt to characterize the fatigue response of arteries. The literature did not provide much information regarding the fatigue response of arteries. In the future, a more intricate three layered model for the artery could be developed and it would more appropriately represent the actual structure of the artery. Moreover, the elastin and collagen fibers within the artery are arranged in the form of a composite structure which could also be implemented in the arterial modeling.

The artery was assumed to be non linear elastic material. Arteries have also been modeled as hyperelastic and viscoelastic material. The fatigue response of arteries is also dependant on the material properties of the artery. There are, therefore, for investigating the artery using a model made of hyperelastic or viscoelastic material.

REFERENCES

1. Stress-Life fatigue Analysis: ETBX. http://www.feaoptimization.com/ETBX/stresslife_help.html
2. Suresh,S., Fatigue of Materials. Second ed 1998. Cambridge University Press.
3. Harris,B., Fatigue in Composites. 2003. Woodhead Publishing Ltd.
4. Rabinowitz,S., Breadmore,P., Cyclic deformation and fracture of polymers. 1974. Journal of Material Sciences (9), 81-99
5. De Santis,R .,Sarracino ,F.,. Mollica,F .,Netti ,P.A.,Ambrosio,L.,Nicolais,L., Continuous fiber reinforced polymers as connective tissue replacement.2004.Composite science and Technology (4),861-871.
6. Liao.D.,Zhao.J., Kunwald.P., Gregerse.H Tissue softening of guinea pig oesophagus tested by the tri-axial test machine
7. Introductory Biomechanics: From Cells to Organisms. C. Ross Ethier and Craig A. Simmons.
8. http://www.engin.umich.edu/class/bme456/cartilage/cart.htm. Cartilage Structure and function.
9. McCord B. 1993. Fatigue of Atherosclerotic Plaque. Georgia Institute of technology, 154.
10. Ku D.N, Greene P.R. 1981. Scleral Creep in Vitro Resulting from Cyclic Pressure Pulses: Applications to Myopia. American Journal of Optometry and Physiological Optics. 58(7): 528-535.
11. Wang X.T, Robert F.Ker, McNeill R.A. 1995. Fatigue rupture of wallaby tail tendon. The Journal of Experimental Biology. 198: 847–852.

12. Schechtman H, Bader D.L. 1997. In vitro fatigue of human tendons. Journal of Biomechanics. 30(8): 829-835.
13. Robert F.Ker, Xiao Tong Wang and Anna V.L Pike.2000. Fatigue quality of Mammalian tendons. The Journal of Experimental Biology 203, 1317–1327.
14. Weightman. B. 2004. Tensile fatigue of Human articular cartilage. Journal of Biomechanics. 9(4): 193-200.
15. Bellucci G, Seedhom B.B. 2001. Mechanical behavior of articular cartilage under tensile cyclic load. Rheumatology. 40: 1337-1345.
16. Broom N.D.1977. The Stress/Strain and Fatigue Behavior of Glutaraldehyde Preserved Heart-Valve Tissue. Journal of Biomechanics. 10: 707-724.
17. Wells S.M, Sacks, M.S. 2001. Effects of fixation pressure on the biaxial mechanical behavior of porcine bioprosthetic heart valves with long-term cyclic loading. Journal of Biomaterials. 23: 2389-2399.
18. Yokobori A.T, Maeyama T, Ohkum T, Yokobori T. 1986. Bio-Medico-Mechanical Behavior of Natural Artery Blood Vessel under Constant and Variable Internal Pulsatile Pressure Flow Test In Vitro. Journal of Biomechanical Engineering. 108: 295-300.
19. Gilpin C.M. 2005. Cyclic loading of Porcine coronary artery (Thesis). Georgia Institute of Technology.
20. Transport in Mammals. http://www.s-cool.co.uk/a-level/biology/transport/revise-it/transport-in-mammals
21. Robert F.Ker, Xiao Tong Wang and Anna V.L Pike.2000. Fatigue quality of Mammalian tendons. The Journal of Experimental Biology 203, 1317–1327.

22. Glagov S, Vito R, Giddens D.P,Zarins C.K.1992.Micro-architecture and composition of artery walls: relationship to location, diameter and the distribution of mechanical stress. Journal of Hypertension 10,101-104.
23. Dobrin P.B.1978. Mechanical properties of arteries. Physiological Reviews 58.
24. Science daily,article Nov 15th ,2006: Math model could Aid study of Collagen Ailments. http://www.sciencedaily.com/releases/2006/11/061114190020.htm
25. Reuterwall O.P.1921.Uber DIE Elastizitat der Gefaswande und die Methode ihrer nabereb Prufung.Acta Med.Scand,Suppl 2,1-175.
26. Roach M.R, Burton A.C.1957. The reason for the shape of the distensibility curves of arteries. Journal of Biochemistry and Physiology 35,681-690.
27. Wolinsky H, Glagov S.1964. Structural basis for the static mechanical properties of the aorta media. Circulation Research 14,400-413.
28. Peterson L.H, Jensen R.E, Parnell R. 1960. Mechanical properties of arteries in vivo. Circulation Research 8, 622-639.
29. Wiedermielm C.A.1965. Distensibility characteristic of small blood vessels.Federation Proceeding Journal 24, 1075-1084.
30. Browell R.2006. ANSYS Fatigue Module tutorial: Calculating and Displaying Fatigue Results. ANSYS Inc.
31. Armentano R, Megnien J.L, Simon A, Bellenfant F, Barra J, Levenson J. 1995. Effects of Hypertension on viscoelasticty of carotid and femoral arteries of human. AHA: Hypertension. 26:48-54.
32. Sharma M.G, Hollis T.M. 1975. Rheological properties of arteries under normal and experimental hypertension. Journal of Biomechanics. 9(5): 293-300.

33. Hu J.J, Fossum T.W, Miller M.W, Xu H, Liu J.C, Humphrey J.D. 2007. Biomechanics of Porcine Basilar Artery in hypertension. Annals of Biomedical Engineering. 35(1): 19-25.
34. Lichtenstein O, Safar M.E, Mathieu E, Poitevin P, Levy B.I. 1998. Static and Dynamic Mechanical Properties of the Carotid Artery From Normotensive and Hypertensive Rats. Hypertension 32,346-350.
35. Intengan H.D, Schiffri E.L. 2000. Structure and Mechanical Properties of Resistance Arteries in Hypertension. Role of Adhesion Molecules and Extracellular Matrix Determinants. Hypertension 36,312-31.
36. Ozolanta I, Tetere G, Purinya B, Kasyanov V. 1998. Changes in the mechanical properties, biochemical contents and wall structure of the human coronary arteries with age and sex. Medical Engineering & Physics 20, 523–533.
37. Van der Heijden-Spek J.J, Staessen J.A, Fagard R.H, Hoeks A.P, Boudier H.A.S, Van Bortel L.M.2000. Effect of Age on Brachial Artery Wall Properties Differs From the Aorta and Is Gender Dependent A Population Study. Hypertension 35, 637-642.
38. Cameron J.D, Bulpitt C.J, Pinto E.S, Rajkumar C. 2003. The Aging of Elastic and Muscular Arteries A comparison of diabetic and non diabetic subjects. Diabetes Care 267, 2133-2138.
39. Reddy A.K, Li Y.H, Pham T.T, Ochoa L.N, Trevin˜ o M.T, Hartley C.J, Lloyd M.H,. Entman M.L and Taffet G.E.2003. Measurement of aortic input impedance in mice: effects of age on aortic stiffness American Journal of Physiology - Heart and Circulatory Physiology 285, H1464–H1470.

40. Han H.C.2007. A biomechanical model of artery undulation. Journal of Biomechanics 40, 3672-3678.

41. Han H.C.2008. Nonlinear undulation of Blood vessels: A theoretical study. Journal of Biomechanics 41, 2708-2713.

42. X. Zhang and J. F. Greenleaf.2006. The stiffening of arteries by the tissue-mimicking Gelatin. IEEE transactions on ultrasonics, ferroelectrics, and frequency control 53, 1534-1539.

43. Restrepom M.B. 2010. Ultrasound Study of the Mechanical Properties of the Arterial Wall. Thesis submitted to Mayo Graduate school, College of Medicine.

44. ANSYS Workbench Version 12.1.

45. McLoughlin R, Dolan F, Lally C, Prendergast P.J. 2006. Tensile and Fatigue testing of porcine coronary arteries in the longitudinal and circumferential directions. Presented at Scientific Advisory Board Review.

46. Ariduru.L.2004.Fatigue life calculation by Rainflow cycle counting Method. Thesis submitted to the Middle East Technical University.

47. Laurent S, Girerd X, Mourad JJ, Lacolley P, Beck L, Boutouyrie P, Mignot JP, Safar M.1994. Elastic modulus of the radial artery wall material is not increased in patients with essential hypertension. Arteriosclerosis, Thrombosis, and Vascular Biology 14, 1223-31.

48. Lally C, Reid A.J and Prendergast P.J. Elastic Behavior of Porcine Coronary Artery Tissue Under Uniaxial and Equibiaxial Tension Annals of Biomedical Engineering 32, 1355-1364.

49. McLoughlin R, Dolan F, Lally C, Prendergast P.J. 2006.Tensile and fatigue testing of porcine coronary arteries in the longitudinal and circumferential direction. Presented at Scientific Advisory Board Review.
50. Sarkar.S, Majumder.S, Roychowdhury.A.2004. Response of human head under static and dynamic load using finite element method. Trends in Biomaterials and Artificial Organs 17,130-134.
51. Cloot R.J.H.2007. Biomechanics of Traumatic Brain Injury: Influences of the Morphologic Heterogeneities of the Cerebral Cortex. Thesis submitted to Eindhoven University of Technology.
52. Wolinsky H, Glagov S.1976. A lamellar unit of aortic medical structure and function in mammals. Circulation Research 20, 99-111.
53. Clarke D, Glagov S.1985. Transmural organization of the arterial media. The lamellar unit revisited. Arteriosclerosis 5, 19-34.
54. O'Rourke M.F, Avolio A.P, Lauren P.D, Yong J.1987. Age related changes of elastic lamellae in the human thoracic aorta. Journal of American college of cardiology 9,53A.
55. O'Rourke M.1990.Arterial stiffness, systolic blood pressure and logical treatment of arterial hypertension. Hypertension 15,339-347.
56. Pourageaud F, Crabos M, Freslon J.L.1997. The elastic modulus of conductance coronary arteries from spontaneously hypertensive rats is increased. Journal of Hypertension 15, 1113-1121.

57. Astrand H, Ahigren A.R, Sandgren T, Lanne T. 2005. Age-related increase in wall stress of the human abdominal aorta: An in vivo study. Journal of Vascular surgery 42, 926-931.

58. Samijo S.K, J.M. Willigers J.M, Barkhuysen R , Kitslaar P.J.E.H.M, Reneman R.S, Brands P.J , Hoeksa A.P.G. 1998. Wall shear stress in the human common carotid artery as function of age and gender. Cardiovascular Research 39, 515-522.

59. Weaver JPA, Evans A, Walder DN.1969. The effect of increased fibrinoflow change in the canine carotid artery. Am J Physiol gen content on the viscosity of blood. Clin Sci 36,1–10.

60. Han H.C.2007. A biomechanical model of artery undulation. Journal of Biomechanics 40, 3672-3678.

61. Johnston B.M and Johnston P.R. 2007.The relative effects of arterial curvature and lumen diameter on wall shear stress distributions in human right coronary arteries. Physics in Medicine and Biology 52, 2531–2544

62. Hodis S, Zamir M.2009. Mechanical events within the arterial wall: The dynamic context for elastin fatigue. Journal of Biomechanics 42, 1010-1016.

63. Han H.C.2009.Blood vessel undulation within soft surrounding tissue generates tortuosity. Journal of Biomechanics 42, 2797-2801.

64. Restrepo M.B.2010.Ultrasound study of the Mechanical properties of the Arterial Wall. A thesis submitted to the faculty of Mayo Clinic.

65. Zhang X, Greenleaf J.F.2006. The stiffening of arteries by the Tissue-mimicking Gelatin. IEEE Transactions on ultrasonics, ferroelectrics and frequency control 53,1534-1549.